https://doi.org/10.5194/egusphere-2026-1040
Preprint. Discussion started: 10 March 2026

Net primary productivity in the Gulf of California: spatiotemporal patterns and drivers in a warming climate (2003–2024)

Eduardo González-Rodríguez[1], Juan David Acevedo-Acosta[2], Rafael Cervantes-Duarte[2], and Jaime Gómez-Gutiérrez[2]

[1]Centro de Investigación Científica y de Educación Superior de Ensenada, Unidad Académica La Paz, Miraflores 334, La Paz, Baja California Sur, C.P. 23050, Mexico
[2]Instituto Politécnico Nacional, Centro Interdisciplinario de Ciencias Marinas, Av. Instituto Politécnico Nacional s/n, Col. Playa Palo de Santa Rita, La Paz, Baja California Sur, C.P. 23096, Mexico

Correspondence to: Juan David Acevedo-Acosta juandavid-88@hotmail.com

Abstract. The Gulf of California is a highly productive ecosystem that supports approximately 70 % of Mexico's fisheries. Despite its ecological and socio-economic importance, few studies have examined the basin-scale seasonal and interannual variations in net primary productivity (NPP). This study analyses 22 years (2003–2024) of satellite-derived NPP data to identify its main spatiotemporal patterns and environmental drivers. The monthly climatology reveals that the cold season (December–May) accounts for 68 % of the annual NPP, while the warm season (June–November) contributes only 32 %. To characterize regional variability, we applied the k-means++ clustering algorithm, validating the classification with discriminant analysis. This procedure robustly identified three productivity zones: high (HPZ; > 1700 mg C m^{-2} d^{-1}), mid (MPZ; 900–1700 mg C m^{-2} d^{-1})mid (MPZ; 900–1700 mg C m^{-2} d^{-1}), and low (LPZ; < 900 mg C m^{-2} d^{-1}). Interannually, the HPZ contributes 61.4 % of the total NPP while covering only 30 % of the gulf's area, whereas the LPZ covers 36 % of the area but contributes just 16.9 %. A significant negative anomaly between 2013 and 2019 led to a 9 % decline in NPP relative to the long-term mean (124 Tg C y^{-1}), a period that included intense warming episodes, including multiple marine heatwaves and the strong 2015–2016 El Niño. A partial recovery was observed from 2020 to 2024. The dominant environmental drivers of NPP differ among zones: sea surface temperature and mixed-layer depth dominate in the HPZ, temperature and euphotic zone depth in the MPZ, and euphotic depth and phosphate availability in the LPZ. Our analysis demonstrates that anomalously warm years reduce the spatial extent of productive zones. As ocean warming and stratification persist, oligotrophic conditions are likely to expand, increasing the coverage of low-productivity waters within the gulf with profound ecological consequences for the Gulf of California.

1 Introduction

The Gulf of California is a highly diverse ecosystem that supports approximately 70 % of Mexico's fisheries (Lluch-Cota et al., 2007). This gulf is influenced by multiple atmospheric and oceanic processes that complicate the characterization of this complex marine system (Kahru et al., 2004; Bustos-Serrano and Castro-Valdez, 2006; Lopez-Martinez et al., 2023; Marin-Enriquez et al., 2024). Among these processes, prolonged anomalous warming of the surface ocean exerts widespread negative

https://doi.org/10.5194/egusphere-2026-1040
Preprint. Discussion started: 10 March 2026

impacts on marine ecosystems, with large-scale repercussions for ecological and biogeochemical functioning (Somavilla et al., 2017). Such events can alter particulate carbon flux (Xie et al., 2019), reduce biodiversity (Wernberg et al., 2016; Jones et al., 2018), and affect fisheries and aquaculture (Mills et al., 2013; Oliver et al., 2017). Enhanced ocean-atmosphere heat exchange during warming events strengthens water-column stratification (Jacox et al., 2016; Somavilla et al., 2017), disrupting nutrient supply and driving changes throughout marine food webs (Cavole et al., 2016). For instance, reductions in phytoplankton biomass and primary productivity have been documented during anomalous warming episodes such as El Niño events (Jacox et al., 2016).

Despite ongoing global warming, the response of oceans and marine ecosystems to changing sea temperature patterns remains uncertain (Somavilla et al., 2017). In recent decades, anomalous warming events, including the positive phase of El Niño–Southern Oscillation (ENSO) and marine heatwaves, have increased in frequency across multiple ocean regions (Di Lorenzo and Mantua, 2016; Oliver et al., 2019). These events produce positive sea surface temperature (SST) anomalies over a range of spatial and temporal scales and are generally associated with declines in primary productivity (Wernberg et al., 2016; Oliver et al., 2017). Concurrently, global ocean heat content has risen over the past five decades (NOAA, https://www.ncei.noaa.gov/access/global-ocean-heat-content/), suggesting that marine ecosystems may be approaching resilience thresholds with potentially irreversible consequences (Froelicher et al., 2018).

The northeastern Pacific Ocean represents a transitional marine ecosystem (Fiedler and Talley, 2006; Cepeda-Morales et al., 2013), where warming events across diverse spatiotemporal scales have been reported in the Gulf of California (Sanchez-Cabeza et al., 2022; Lopez-Martinez et al., 2023). Notably, the combined influence of the Blob in the North Pacific, a strong equatorial El Niño event, and overlapping marine heatwaves between 2013 and 2016 produced persistent warm anomalies in northwestern Mexico (Jimenez-Quiroz et al., 2019; Joh and Di Lorenzo, 2017; Garcia-Fernandez et al., 2023). These anomalies propagated through mid and upper trophic levels, altering species distributions, including euphausiids, copepods, pelagic crabs, and tunas, in the Eastern Tropical Pacific (Cavole et al., 2016; Garcia-Fernandez et al., 2023). As global temperatures rise, such anomalies are expected to disrupt the biological carbon pump, reducing oceanic carbon storage and increasing atmospheric carbon concentrations (Cavole et al., 2016; Xie et al., 2019). These changes will likely reshape community structures and ecosystem functioning (Cavole et al., 2016).

The Gulf of California (20–32° N) is among the most diverse and productive marine regions in Mexico, characterized by high net primary productivity (NPP, defined as gross primary productivity minus respiration) and phytoplankton biomass [chlorophyll-*a* concentration (Chl-*a*)] (Lluch-Cota, 2004; O'Reilly and Sherman, 2016). Its elongate geometry, steep bathymetry, and pronounced orographic relief modulate regional pressure-gradient forcing and orographic channelling of the winds, generating seasonally coherent along-gulf winds whose wind-stress curl drives Ekman upwelling, coastal divergence, and vertical mixing that inject nutrient-rich subsurface waters into the euphotic zone (Miranda-Alvarez et al., 2020; Robles-Tamayo et al., 2020). However, anomalous warming associated with the positive phase of ENSO and the Pacific Decadal Oscillation (PDO) reduces mean Chl-*a* concentration in the gulf (Hakspiel-Segura et al., 2022; Lopez-Martinez et al., 2023). *In situ* NPP measurements in the region remain scarce, particularly during winter, limiting our understanding of the latitudinal gradient and seasonal cycles (Zeitzchel, 1969; Alvarez-Borrego and Lara-Lara, 1991; Mercado-Santana et al., 2017). Remote-sensing estimates of

https://doi.org/10.5194/egusphere-2026-1040
Preprint. Discussion started: 10 March 2026

NPP and Chl-*a*, based on ecological models incorporating light-use efficiency and absorbed photosynthetically active radiation, have partially addressed these gaps. However, most studies have focused on local variability rather than basin-scale dynamics. Furthermore, while satellite-derived Chl-*a* is often used as a proxy for NPP, it reflects biomass within the first optical depth, whereas NPP integrates production across the entire euphotic zone and daylight period (Behrenfeld and Falkowski, 1997).

In this study, we investigate the response of NPP in the Gulf of California to recent anomalous warming events, using a 2003–2024 satellite record to establish the seasonal and interannual baseline against which anomalies are assessed. We specifically focus on the 2013–2024 period, encompassing the 2014–2016 warming event, to evaluate how elevated SSTs and enhanced stratification modify the spatial distribution of productivity and its environmental controls. We hypothesize that anomalous warming events intensify water-column stratification, restricting the flux of nutrient-rich water to the euphotic zone and thereby reducing NPP. By combining satellite observations with reanalysis-based water-column variables, we identify the key drivers that modulate NPP under anomalously warm conditions.

2 Materials and Methods

2.1 Study area

The Gulf of California (32–20º N, 105–115º W) is a marginal subtropical sea of the eastern Pacific located in northwestern Mexico (Fig. 1). It extends ~1,500 km from its northernmost limit to Bahía de Banderas in the south and is 150–200 km wide. South of 28º N, the gulf comprises a series of deep basins separated by bathymetric sills (Alvarez-Borrego and Lara-Lara, 1991). The region exhibits dynamic and heterogeneous conditions driven by tidal currents, wind momentum transfer, bathymetrically controlled and wind-driven coastal upwelling, and intense solar heating (Alvarez-Borrego, 2007). In the Midriff Archipelago, bathymetric upwelling maintains low temperatures year-round. From December to May, northwesterly winds induce strong coastal upwelling along the eastern coast, transporting nutrient-rich subsurface waters into the euphotic zone that fuel phytoplankton growth. In contrast, from July to October, southeasterly winds are generally weaker and insufficient to disrupt the pronounced thermal stratification that develops during summer. June and November are considered transitional months between the cold–warm and warm–cold seasonal regimes (Santamaria-del Angel et al., 1994; Hidalgo-Gonzalez and Alvarez-Borrego, 2004). The Baja California mountain ranges block low-lying clouds from the Pacific Ocean, resulting in predominantly clear skies over the gulf except during summer monsoon incursions (Badan-Dangon et al., 1985). For this study, the southern boundary of the Gulf of California was defined by a line connecting Cabo San Lucas on the Baja California peninsula (23° N) to Cabo Corrientes in Nayarit (~20º N; Fig. 1).

https://doi.org/10.5194/egusphere-2026-1040
Preprint. Discussion started: 10 March 2026

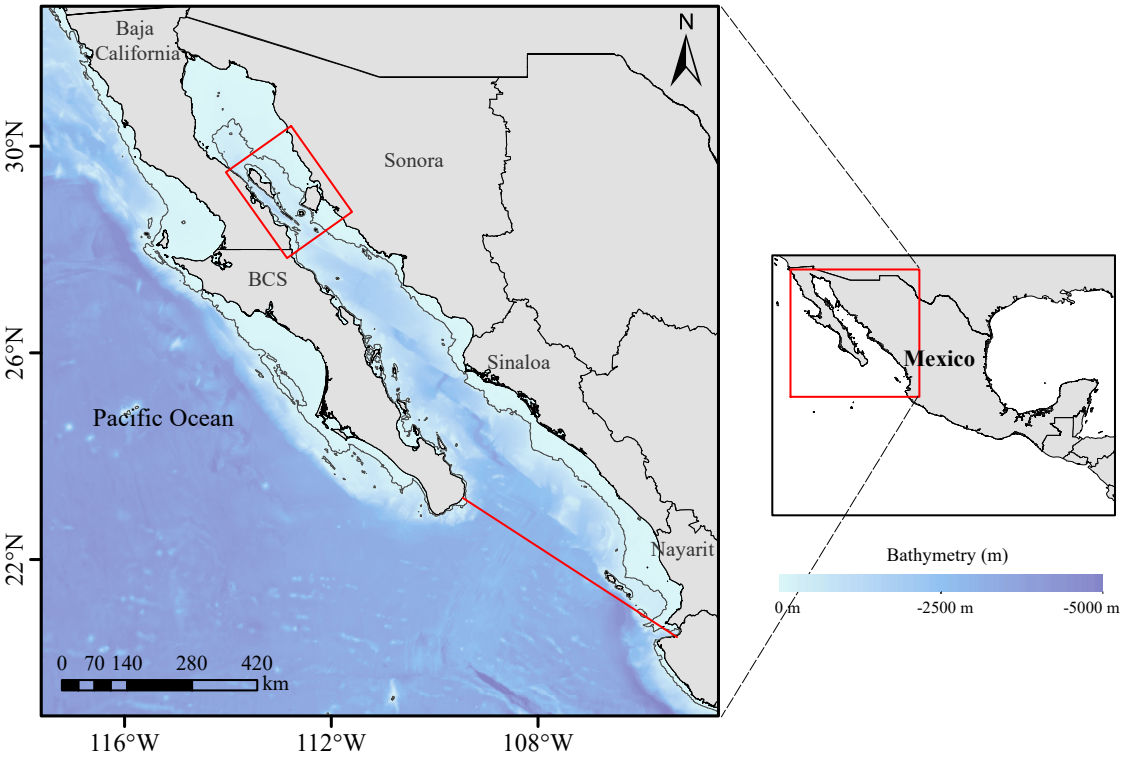

Figure 1. Bathymetric map of the Gulf of California, conceptually delimited from the Pacific Ocean by a red line. The gulf is a large and deep pull-apart basin formed by right-lateral strike-slip motion along faults associated with the San Andreas system. Tectonic opening on the order of 3–6 cm y^{-1} has shaped the oceanic crust underlying most of the basin. The resulting geological configuration supports oceanographic processes that sustain high phytoplankton productivity, with contrasting dynamics along the opposing coasts. Gray line: continental shelf (isobaths of 200 m); red square: Midriff Archipelago region.

2.2 Data collection

2.2.1 Satellite variables

Monthly sea surface temperature (SST) and chlorophyll-*a* concentration (Chl-*a*; OCI algorithm) were obtained from Aqua–MODIS Level-3 global composites (4 × 4 km) spanning January 2003 to December 2024, downloaded from NASA Ocean Color (https://oceancolor.gsfc.nasa.gov/l3/).

Euphotic-zone depth (EZD) was derived from Chl-*a* using the chlorophyll-*a*-dependent bio-optical parameterization with piecewise power-law relationships for different trophic regimes (Morel and Berthon, 1989; Morel and Maritorena, 2001).

Net primary productivity (NPP) at the same nominal resolution (4 × 4 km) was obtained from monthly Level-3 products of the Vertially Generalized Production Model (VGPM) via NOAA CoastWatch (https://coastwatch.pfeg.noaa.gov/erddap/griddap/erdMH1ppmday.graph). Monthly 10-m wind components (u, v) were obtained from the Remote Sensing Systems

https://doi.org/10.5194/egusphere-2026-1040
Preprint. Discussion started: 10 March 2026

(RSS) CCMP V3.1 Level-3 dataset (25 × 25 km) for 2003–2024 (https://data.remss.com/ccmp/v03.1/). To account for the gulf's orientation, the coordinate axes were rotated by 40º, aligning the total u-component with the gulf's axis and the rotated v-component perpendicular to it. The along-gulf wind u-component (URT) was used in statistical analyses.

Daily sea current components (u, v; Level 4; 12.5 × 12.5 km) were obtained from the Copernicus Marine Environment Monitoring Service (CMEMS, https://doi.org/10.48670/moi-00148). Monthly means were computed for 2003–2024 and rotated analogously to the wind components; only the along-gulf u-component (UAR) was used in statistical analyses.

2.2.2 Reanalysis variables and derived parameter

Monthly Global Ocean Biogeochemistry Hindcast reanalysis data (`GLOBAL_REANALYSIS_BIO_001_029`) for nitrate (NO_3), phosphate (PO_4), and silicate (SiO_2) concentrations were downloaded from CMEMS (https://doi.org/10.48670/moi-00019). These Level-4 products are provided on a 25 × 25 km grid with 75 depth levels. Mixed layer depth (MLD), potential temperature (θ), and practical salinity (PSU) were obtained from the Global Ocean Physics Reanalysis (`GLOBAL_REANALYSIS_PHY_001_030`) at ∼8 × 8 km horizontal resolution with 50 standard depth levels (https://doi.org/10.48670/moi-00021/).

2.2.3 Data homogenization

To ensure consistency, NO_3, PO_4, SiO_2, MLD, and the stratification index described in Section 2.3.2 were bilinearly interpolated to the 4 km grid used for NPP, SST, and EZD. Only grid cells within the Gulf of California domain (Fig. 1) were retained for analyses.

2.3 Data processing

2.3.1 Identification of warm events, climate indices and spatial trends

Anomalous warm periods were identified using SST anomalies (SSTa), and marine heatwaves (MHWs) were detected following (Hobday et al., 2016), who define MHWs as periods when SST exceeds a seasonally varying 90th-percentile threshold for ≥ 5 consecutive days.

The bimonthly Multivariate ENSO Index version 2 (MEI v2) was used to track ENSO evolution and strength. MEI v2 integrates sea-level pressure, sea surface temperature, zonal and meridional surface winds, and outgoing longwave radiation using empirical orthogonal functions (EOFs) over the tropical Pacific (30° S to 30° N) (Wolter and Timlin, 2011; Kobayashi et al., 2015). MEI v2 data were downloaded from the National Oceanic and Atmospheric Administration (https://psl.noaa.gov/enso/mei/) for the entire study period. ENSO influence was assessed by comparing SST anomaly (SSTa) time series with MEI v2 (Fig. 2). Spearman's rank correlations were computed among hydrographic variables, climate indices, and NPP across gulf regions. Spatial trends were estimated using the `Trend` function from the Climate Data Toolbox for MATLAB (Greene et al., 2019), which applies least-squares regression to time-series data.

https://doi.org/10.5194/egusphere-2026-1040
Preprint. Discussion started: 10 March 2026

2.3.2 Calculation of stratification index

Water-column stratification was quantified using a density-based index calculated from vertical profiles of potential temperature (θ) and practical salinity (PSU). The stratification index (SI; kg m^{-3}) was defined as the difference between potential density at the surface and at the base of the mixed layer depth:

$$\mathrm{SI} = \sigma_{\theta,\mathrm{surface}} - \sigma_{\theta,\mathrm{MLD}} \tag{1}$$

where σ_θ is potential density referenced to 0 dbar. Practical salinity was first converted to absolute salinity (g kg^{-1}), accounting for latitude, longitude, and pressure. Potential density was then calculated at the surface (0 m) and at the MLD using the TEOS-10 equation of state (Intergovernmental Oceanographic Commission, 2010). With this definition, positive SI values indicate stable stratification (lighter surface waters overlying denser subsurface waters), whereas values near zero denote well-mixed conditions. This index represents the physical barrier to vertical mixing, linking surface warming to reduced nutrient supply (Jacox et al., 2016).

2.3.3 Regional classification of net primary productivity

To analyse spatiotemporal variability, monthly NPP fields from January 2003 to December 2024 were classified into zones. Outliers were removed following (Moore and McCabe, 1999). NPP was then grouped into three clusters using the k-means++ algorithm (Kapoor and Singhal, 2017; Zhang et al., 2025).

Discriminant analysis (Johnson and Wichern, 2018) was applied to all variables except NPP to validate cluster assignments. Spatial distribution and seasonal patterns (cold season: December–May; warm season: June–November) were visualized (Santamaria-del Angel et al., 1994; Hidalgo-Gonzalez and Alvarez-Borrego, 2004).

The areal coverage for each cluster was calculated by counting grid cells within each class, converting to km^2, and then to percentage coverage (%) per month, season, and year. Monthly anomalies were calculated from the coverage time series (Kushnir, 1994; Ramos-Rodriguez et al., 2012).

Monthly climatological NPP was estimated for each cluster, and cluster contributions were integrated to obtain total monthly productivity. NPP was expressed in teragrams of carbon per month (Tg C month^{-1}) and per year (Tg C y^{-1}). Annual distribution patterns were visualized (Fig. 5; Fig. A1 and Fig. A2).

2.3.4 Assessment of NPP drivers

To explain spatial and temporal variability in NPP, the following biophysical variables were analysed for each NPP zone: SST, EZD, MLD, NO_3, PO_4, SiO_2, URT, UAR, and SI. Monthly time series were computed by zone for each variable. Nutrients (NO_3, PO_4, SiO_2) were vertically integrated from the surface to the EZD prior to analysis.

SST, EZD, and MLD were standardized to derive anomalies. Potential collinearity among predictors was evaluated using correlation matrices; highly correlated variables were excluded from the final predictor set. To evaluate environmental controls

https://doi.org/10.5194/egusphere-2026-1040
Preprint. Discussion started: 10 March 2026

on NPP while accounting for spatial heterogeneity among zones, a generalized linear mixed model (GLMM) with Gaussian errors was fitted. Fixed-effect coefficients (estimate, standard error, t-statistic, and p-value) were evaluated with marginal ANOVA to identify significant predictors and interaction terms. Predictors with $p < 0.05$ were considered significant drivers of NPP. Positive coefficients indicate that higher predictor values are associated with increased NPP, whereas negative coefficients suggest inhibitory or limiting effects. The model structure was:

$$\mathrm{NPP} = \mathrm{Zone} \times (\mathrm{SST} + \mathrm{EZD} + \mathrm{MLD} + \mathrm{NO_3} + \mathrm{PO_4} + \mathrm{SiO_2} + \mathrm{URT} + \mathrm{UAR} + \mathrm{SI}) \quad (2)$$

3 Results

3.1 Anomalous warming events

Sea surface temperature anomalies (SSTa) in the Gulf of California were predominantly negative from 2003 to 2013. Beginning in 2014, anomalies transitioned to positive values, with increasing frequency and duration over time. The most intense and persistent positive anomalies occurred between late–2013 and late–2016 (Fig. 2a).

During 2014–2016, the annual number of MHW days reached 118, 95, and 51 days, respectively, representing 50.2% of all MHW days in the 2003–2024 record (Fig. 2b). The MEI v2 also showed strong positive anomalies and extreme values during 2015–2016, consistent with the 2015–2016 El Niño event, and was flanked by prolonged negative anomalies associated with La Niña conditions during 2010–2014 and 2016–2018 (Fig. 2c).

Taken together, SSTa, MHW occurrence, and MEI v2 indicate that the warmest period of the study was 2014–2016, followed by 2023–2024, which recorded the second-highest number of MHW days.

3.2 Regional classification of net primary productivity

The k-means++ clustering analysis identified three groups based on NPP, with only 8.7 % of observations (51,572 out of 591,836 records) misclassified. Classification accuracies for the three groups were 92.4 %, 96.1 %, and 80.1 %, respectively. These groups were categorized as low (LPZ, < 900 mg C m^{-2} d^{-1}), mid (MPZ, 900–1700 mg C m^{-2} d^{-1}), and high (HPZ, $>$ 1700 mg C m^{-2} d^{-1}) productivity zones (Fig. 3). This regionalization provides the spatial framework to assess how anomalous warming modifies the extent, contribution, and environmental controls of productivity across the gulf.

3.3 Intra- and interannual variability of primary productivity

The 2003–2024 NPP climatology ranged from 642 to 3487 mg C m^{-2} d^{-1}. The average annual spatial pattern showed a longitudinal gradient along the continental coast, extending from the gulf mouth (~20° N) to the northern gulf (~31.5° N). The most productive regions (HPZ, > 1700 mg C m^{-2} d^{-1}) included the Nayarit, Sinaloa, and Sonora coasts, the Midriff Archipelago (28° N; 1200–2000 mg C m^{-2} d^{-1}), and the Colorado River mouth extending ~40 km offshore.

https://doi.org/10.5194/egusphere-2026-1040
Preprint. Discussion started: 10 March 2026

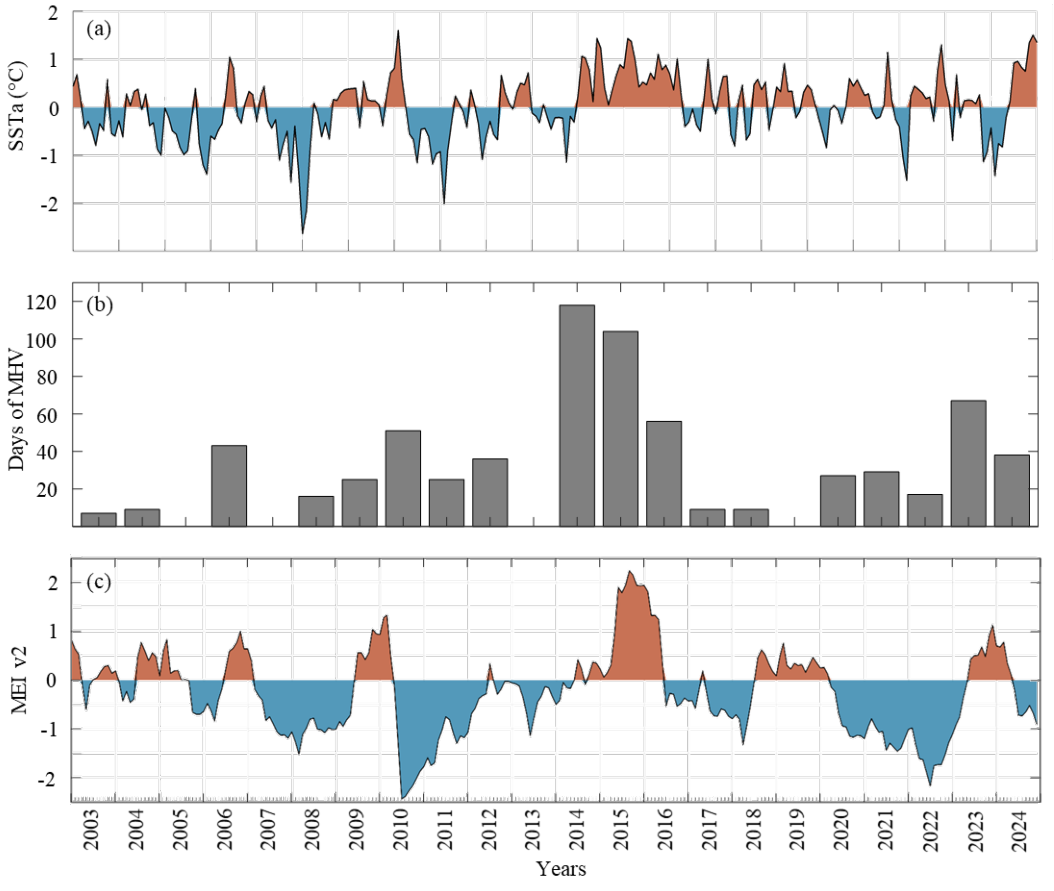

Figure 2. Time series for the Gulf of California showing (a) monthly sea surface temperature anomaly (SSTa), (b) annual number of marine heatwave (MHW) days, and (c) the Multivariate ENSO Index version 2 (MEI v2) from January 2003 to December 2024.

Intermediate productivity (MPZ, 900–1700 mg C m^{-2} d^{-1}) occupied coastal waters near the gulf mouth and southern sector, forming a coast-to-shelf gradient. The MPZ extended from ~25° N to the Midriff Archipelago region and along the entire peninsular coast, with a core in the upper gulf. Low productivity waters (LPZ, < 900 mg C m^{-2} d^{-1}) characterized oligotrophic conditions from the gulf mouth to ~26° N (Fig. 3a). Seasonality was pronounced. During the warm period (June–November), HPZ and MPZ coverage decreased, while LPZ expanded northward to ~28° N, forming a core in the upper gulf (Fig. 3b). In contrast, during the cold period (December–May), HPZ expanded across the upper gulf and along both continental and peninsular coasts (Fig. 3c).

https://doi.org/10.5194/egusphere-2026-1040
Preprint. Discussion started: 10 March 2026

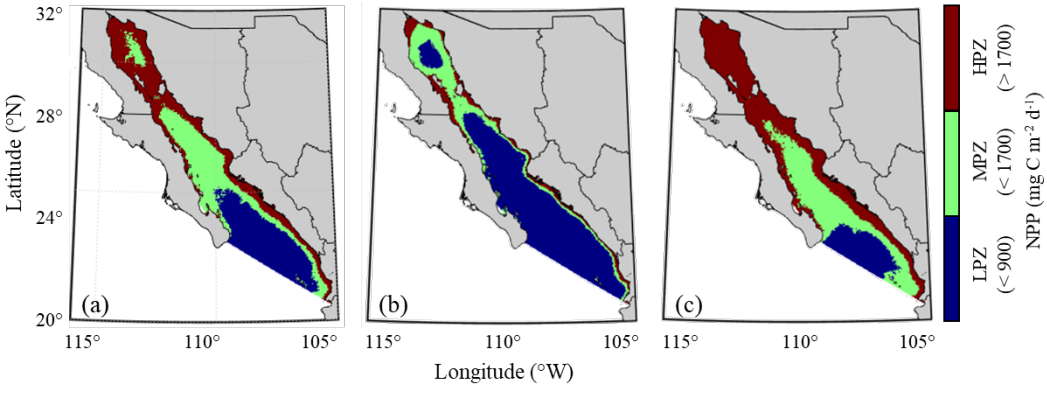

Figure 3. Regionalization of net primary productivity (NPP) based on (a) k-means++ clustering of the 2003–2024 climatology, (b) the warm season (June–November), and (c) the cold season (December–May). NPP classes: low (LPZ < 900 mg C m^{-2} d^{-1}), mid (MPZ 900–1700 mg C m^{-2} d^{-1}), and high (HPZ > 1700 mg C m^{-2} d^{-1}).

Gulf-wide monthly mean productivity was 8.6 Tg C $month^{-1}$. During the cold season, NPP averaged 11.7 Tg C $month^{-1}$, peaking in March at 14.9 Tg C $month^{-1}$. During the warm season, NPP averaged 5.5 Tg C $month^{-1}$, with a minimum in August (4.4 Tg C $month^{-1}$). HPZ coverage increased from 34 to 71 % (mean 54 %) in winter but declined to 19 % in summer, reaching ~8 % in July–August (Fig. 3c and Fig. 4a). LPZ covered 8–20 % (~10 %) in winter and expanded to 49 % in summer, peaking near 66 % in July–August. MPZ accounted for ~34 % annually (Fig. 3b and Fig. 4a).

Annual, zone-integrated NPP ranged from 84 to 198 Tg C y^{-1} (mean 124 ± 27.3 Tg C y^{-1}). Contributions over the entire period were HPZ = 61.4 %, MPZ = 21.6 %, and LPZ = 16.9 % (Fig. 4b). During 2003–2012 (predominantly negative SSTa), HPZ contributed 63.9 %, MPZ 20.9 %, and LPZ 15.1 %. During 2013–2024 (positive SSTa), LPZ increased to 18.4 %, while HPZ declined to 59.4 %, indicating a progressive reduction in HPZ extent, whereas MPZ remained stable at ~21.6 %.

Years 2006–2012 exceeded the historical mean, with 2008, 2011, and 2012 being the most productive (167, 198, and 164 Tg C y^{-1}, respectively). In those years, HPZ contributed ~78 % of NPP, while LPZ contributed 14–17 %. In contrast, the anomalously warm interval (2014–2016) recorded the lowest mean NPP (~101 Tg C y^{-1}), with LPZ contributing 21.8 % and HPZ declining to 54.7 % in 2016. MPZ exceeded 25 % of NPP in 2004, 2013, 2018, and 2021 (Fig. 4b). The longest below-average period occurred from 2013–2019, followed by recovery during 2020–2024; only 2023 (111 Tg C y^{-1}) remained below the mean. Notably, 2024 ranked as the fourth most productive year (152 Tg C y^{-1}), following 2008, 2011, and 2012.

https://doi.org/10.5194/egusphere-2026-1040
Preprint. Discussion started: 10 March 2026

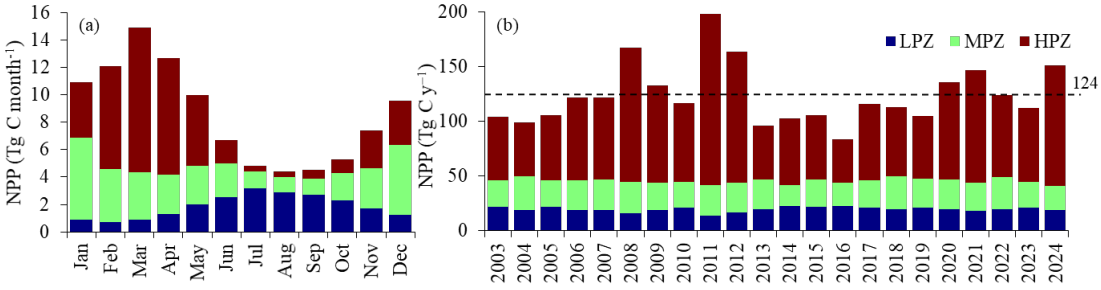

Figure 4. (a) Monthly mean net primary productivity (NPP; bars) from January 2003 to December 2024. Stacked bars show zone contributions (%), and total NPP is expressed in Tg C month^{-1}. (b) Mean annual NPP (Tg C y^{-1}) per zone for 2003–2024. The dashed line indicates the mean annual NPP for the full study period.

3.4 Spatial and interannual variability of primary productivity

The annual spatial distribution of the LPZ, MPZ, and HPZ (Fig. 4) exhibited distinct patterns closely tied to temperature regimes. During 2003–2012, when SST anomalies were predominantly negative, LPZ was mostly located south of 26° N, covering on average 32.4 % of the gulf. In these years, HPZ was prominent in the upper gulf, the Midriff Archipelago region, and along the continental coast, extending $>$ 40 km offshore and accounting for 33.3 % of the area. In contrast, during 2013–2023, when SST anomalies were mostly positive, HPZ coverage decreased markedly in coastal areas and the upper gulf ($<$ 26 % of the area), while MPZ expanded to approximately 33.9 %, occupying much of the basin. The most pronounced spatial reorganization occurred during the anomalously warm period of 2014–2016, when LPZ increased to nearly 50 %, advanced north of 26° N, and reached ~28° N in 2016. Years with widespread HPZ coverage (e.g., 2008, 2011, 2012, 2021, and 2024) coincided with positive NPP anomalies exceeding 25 %, whereas 2013–2016 showed LPZ expansions greater than 20 % (Fig. 5).

Seasonality was most pronounced during the cold period (December–May). On average, HPZ covered 44.2 % of the gulf, followed by MPZ (33.5 %) and LPZ (22.2 %). HPZ coverage ranged from 22.9 % in 2016 to 63 % in 2012, MPZ from 25.7 % (2010) to 42.5 % (2013), and LPZ from 2 % (2021) to 44 % (2016). HPZ exceeded 50 % in 2008 (58 %), 2011 (61.4 %), 2012 (63 %), and 2021 (59.7 %), with LPZ nearly absent ($<$ 10 %) in 2021. Conversely, HPZ fell below the historical average in 2014, reaching 22.9 % in 2016 and 42 % in 2017 (Fig. A1).

During the warm period (June–November), interannual variability was lower. LPZ dominated, averaging 68.5 % coverage (range: 57.9–76.2 %), and shifted northward into the upper gulf. MPZ averaged 19.7 % (15.6–26.9 %), and HPZ averaged 11.7 % (7–22 %), concentrated near the Midriff Archipelago, Colorado River mouth, and along the continental coast, with

https://doi.org/10.5194/egusphere-2026-1040
Preprint. Discussion started: 10 March 2026

limited offshore extent (Fig. A2). Additional latitude–time distributions of NPP and anomalies are shown in Figure A3 and Figure A4.

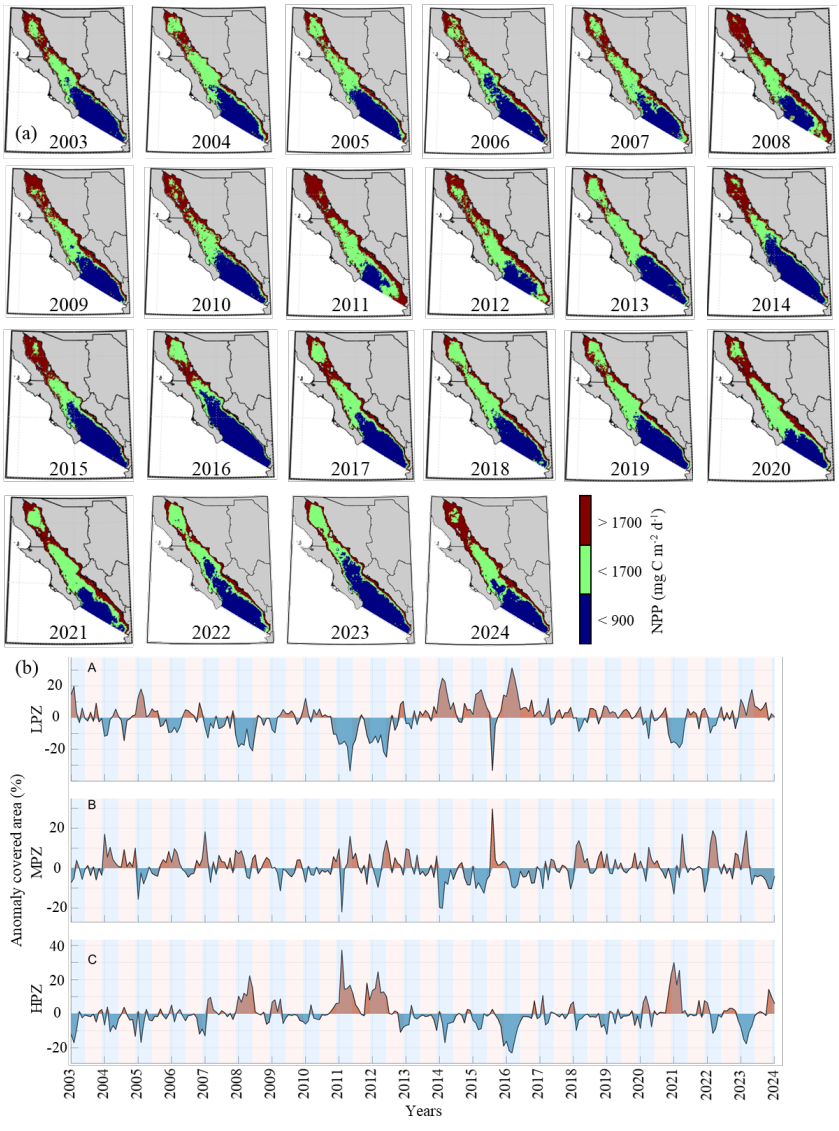

Figure 5. (a) Annual spatial distribution of high (HPZ), mid (MPZ), and low (LPZ) NPP zones from 2003 to 2024; (b) time series of anomalies in class coverage (%) relative to the long-term mean distribution. Blue indicates reductions in coverage, whereas red indicates increases. The shaded box highlights the prolonged anomalously warm period (2014–2016) in the Gulf of California.

https://doi.org/10.5194/egusphere-2026-1040
Preprint. Discussion started: 10 March 2026

3.5 Responses of biophysical drivers (GLMM analysis)

Correlation analysis revealed strong collinearity between PO_4 and SiO_2 ($r = 0.88$; $p < 0.05$). PO_4 was retained in the model because of its broader relevance to primary productivity, whereas SiO_2 primarily constrains siliceous phytoplankton such as diatoms. The best-fitting generalized linear mixed models (GLMMs) for each NPP class identified the significant environmental drivers (Fig. 1).

Main drivers of NPP varied markedly among zones of the Gulf of California. Sea surface temperature (SST) was the dominant predictor. In the LPZ, SST showed a positive but marginally non-significant effect on NPP ($\beta = 0.124$, $p = 0.057$). In the MPZ and HPZ, SST had a significant negative effect on NPP (MPZ: $\beta = -0.338$; HPZ: $\beta = -1.189$; $p < 0.01$).

Within the HPZ, NPP decreased with increasing SST and a deeper mixed layer depth ($\beta = -0.453$, $p < 0.01$), but increased with greater euphotic-zone depth ($\beta = 0.775$, $p < 0.01$) and higher PO_4 concentrations ($\beta = 0.192$, $p < 0.01$). Nitrate, current and wind components (UAR and URT), and stratification index (SI) showed no significant effects in any zone at $\alpha = 0.05$.

The complete anomaly time series for all variables from 2003–2024 is provided in the supplementary material (Fig. A4–Fig. A7). These results underscore strong regional differences in environmental controls on NPP across the Gulf of California.

Overall, the results indicate that anomalously warm conditions reduce the spatial extent and contribution of high-productivity waters while promoting the expansion of oligotrophic conditions, highlighting the strong sensitivity of Gulf of California productivity to thermal variability.

4 Discussion

Monitoring net primary productivity (NPP) in the Gulf of California is essential for assessing the impacts of climate variability and anthropogenic pressures, and their ecological and socioeconomic consequences. NPP underpins fisheries, mediates carbon cycling, and contributes to ecosystem resilience, making it a key indicator of ocean health. Despite its importance, long-term NPP records, both in situ and satellite-derived, remain limited, constraining assessments of variability from seasonal to interannual scales. The spatial organization of the Gulf of California has been described using diverse regionalization schemes reflecting different criteria. Early classifications were based on biological indicators, such as phytoplankton assemblages in sediments (Round, 1967; Zeitzchel, 1969), or on physical properties, including vertical thermohaline structure (Roden and Emilsson, 1979) and bathymetry (Merrifield and Winant, 1989). With the advent of satellite observations, more detailed classifications emerged, notably the 14-region scheme based on photosynthetic pigments proposed by (Santamaria-del Angel et al., 1994). More recent approaches have increased regional complexity by incorporating multivariate physical–chemical variables and machine learning techniques. These classifications range from simplified latitudinal divisions (north, central, south, and mouth) to schemes with 12–22 regions (Santamaria-del Angel et al., 1994; Kahru et al., 2004; Petatan Ramirez, 2015; Heras-Sanchez et al., 2019; Marin-Enriquez et al., 2024), often relying on satellite chlorophyll-a, bathymetry (Lavin-Peregrina and Marinone-Moschetto, 2003), or multivariate environmental datasets. However, regionalization should be guided by the principle of parsimony, as excessive subdivision without a clear mechanistic basis can limit interpretability. Process-based frameworks that emphasize the controls on productivity are therefore preferable.

https://doi.org/10.5194/egusphere-2026-1040
Preprint. Discussion started: 10 March 2026

Table 1. GLMM results for the main effects of biophysical variables on NPP by zone. Coefficients significant at $p < 0.05$ are shown in bold. Abbreviations: LPZ = low-productivity zone; MPZ = mid-productivity zone; HPZ = high-productivity zone; SST = sea surface temperature; EZD = euphotic-zone depth; MLD = mixed layer depth; NO_3 = nitrate; PO_4 = phosphate; UAR = along-gulf current component; URT = along-gulf wind component; SI = stratification index.

Zone	Driver	Estimate	Std. Error	t-ratio	p-value
LPZ	**Intercept**	**-0.527**	**0.134**	**-3.936**	8.67×10^{-5}
	SST	0.124	0.065	1.908	0.057
	EZD	-0.030	0.086	-0.349	0.727
	MLD	0.021	0.074	0.291	0.771
	NO_3	-0.006	0.226	-0.028	0.977
	PO_4	-0.009	0.043	-0.212	0.832
	UAR	-0.035	1.775	-0.019	0.984
	URT	0.032	0.039	0.812	0.417
	SI	0.242	0.392	0.618	0.536
MPZ	Intercept	0.173	0.149	1.158	0.247
	SST	**-0.338**	**0.094**	**-3.606**	3.21×10^{-4}
	EZD	-0.023	0.153	-0.147	0.883
	MLD	0.052	0.084	0.617	0.537
	NO_3	0.027	0.232	0.117	0.907
	PO_4	0.014	0.050	0.276	0.783
	UAR	0.000	2.213	0.000	1.000
	URT	-0.011	0.059	-0.194	0.846
	SI	-0.127	0.455	-0.280	0.780
HPZ	Intercept	-0.146	0.208	-0.702	0.483
	SST	**-1.189**	**0.079**	**-15.092**	3.88×10^{-48}
	EZD	**0.775**	**0.152**	**5.107**	3.68×10^{-7}
	MLD	**-0.453**	**0.093**	**-4.885**	1.14×10^{-6}
	NO_3	0.285	0.226	1.258	0.208
	PO_4	**0.192**	**0.048**	**3.985**	7.06×10^{-5}
	UAR	2.177	1.980	1.100	0.272
	URT	-0.069	0.063	-1.095	0.274
	SI	-0.188	0.406	-0.463	0.644

https://doi.org/10.5194/egusphere-2026-1040
Preprint. Discussion started: 10 March 2026

We applied the K-means++ algorithm because this unsupervised machine learning method optimizes centroid initialization using probabilistic distributions, improving accuracy, reducing iterations, and enhancing convergence stability (Kapoor and Singhal, 2017; Zhang et al., 2025). This approach has proven effective for classifying meteorological and hydrographic patterns (Zhang and Qian, 2025) and primary productivity in the Gulf of California. Our regions align with previous classifications, identifying areas and periods of high, medium, and low NPP.

Our classification defined three NPP categories: HPZ (> 1700 mg C m^{-2} d^{-1}), MPZ (900–1700 mg C m^{-2} d^{-1}), and LPZ (< 900 mg C m^{-2} d^{-1}). HPZ occupies ~30 % of the gulf area but contributes ~61.4 % of total NPP, while LPZ covers ~36 % yet accounts for only ~16.9 %. This latitudinal gradient is consistent with (Gaxiola-Castro et al., 1995), who reported average values ranging from 2.94 (1.98–4.17) g C m^{-2} d^{-1} in the southern Gulf of California to 1.70 (0.64–4.57) g C m^{-2} d^{-1} in the Midriff Archipelago. Similarly, (Valdez-Holguin and Lara-Lara, 1987) reported values between 1.51 and 3.12 g C m^{-2} d^{-1} for central and northern regions.

HPZ typically occur along the eastern continental coast, the Midriff Archipelago, and the upper gulf, where strong mixing and persistent upwelling prevail (Mercado-Santana et al., 2017). In the northwest, tidal currents generate jets and cyclonic eddies that further sustain high productivity (Marin-Enriquez et al., 2024). Seasonal upwelling driven by northwesterly winds along the Sonora, Sinaloa, and Nayarit coasts during winter reinforces these patterns (Santamaria-del Angel et al., 1994; Mercado-Santana et al., 2017).

MPZ contributes ~21 % of total NPP and is characterized by intermediate conditions: SST ~25° C, salinity ~35 psu, and a mixed layer depth ~24 m, with relatively high water-column stability (Marin-Enriquez et al., 2024). This region is influenced by the convergence of Subtropical Subsurface Water (SSW), Tropical Surface Water (TSW), and Gulf of California Water (GCW), which generates fronts, eddies, and mesoscale processes that modulate productivity (Lavin-Peregrina and Marinone-Moschetto, 2003; Lavin et al., 2013).

LPZ corresponds to the most oligotrophic region of the southern gulf, including the Baja California Sur coast, the gulf's mouth, and areas between the continental coast and the Pescadero Basin. Historically, this region exhibits low NPP (0.002–0.95 g C m^{-2} d^{-1}) (Zeitzchel, 1969; Escalante et al., 2013) due to the influence of eastern Pacific waters and the intrusion of warm, low-salinity tropical waters, which intensify stratification and limit nutrient flux to the euphotic zone (Lavin-Peregrina and Marinone-Moschetto, 2003; Mercado-Santana et al., 2017; Marin-Enriquez et al., 2024). The southern gulf's complex thermohaline structure, shaped by GCW, TSW, and California Current Water (CCW), along with mesoscale dynamics (eddies, fronts), further constrain productivity (Lavin-Peregrina and Marinone-Moschetto, 2003; Portela et al., 2016; Marin-Enriquez et al., 2024; Trasviña-Castro et al., 2024).

The GLMM analysis identified SST as the most influential variable controlling NPP in the Gulf of California. This finding aligns with the inverse relationship observed in the annual climatology of NPP and SST, where maximum productivity occurs during the cold season and minimum values during the warm season (Hakspiel-Segura et al., 2022). In HPZ, net primary productivity was additionally influenced by EZD, MLD, and PO_4 concentrations. MLD strongly correlates with nutrient availability (NO_3 and PO_4), consistent with their derivation from a biogeochemical hindcast reanalysis. MLD anomalies showed deeper mixing during cool periods and shoaling during warm stratified conditions (Fig. A6). These factors are particularly

https://doi.org/10.5194/egusphere-2026-1040
Preprint. Discussion started: 10 March 2026

relevant in the upper gulf, the Midriff Archipelago region, and along the eastern continental coast, where bathymetry, tidal currents, and strong northwesterly winds during winter drive intense mixing and persistent upwelling, sustaining productivity (Santamaria-del Angel et al., 1994; Mercado-Santana et al., 2017; Marin-Enriquez et al., 2024).

Although (Alvarez-Borrego, 2012) emphasized nitrogen as the primary limiting nutrient in the gulf, our results indicate that phosphate availability also plays a significant role in regulating NPP, despite its lower stoichiometric requirements. (Millan-Nunez et al., 2023) documented that summer stratification in the Guaymas Basin severely restricts vertical nutrient fluxes, creating nitrogen-limited conditions (NO_3 + NO_2) and reducing surface Chl-a concentrations. These conditions favor dominance of picophytoplankton, which have a higher surface-area-to-volume ratio that enhances nutrient uptake under oligotrophic conditions (Millan-Nunez et al., 2023; Martínez-López et al., 2023). (Browning and Moore, 2023) further noted that co-limitation by nitrogen and phosphorus is common in subtropical environments, including the eastern North Pacific subtropical gyre and the entrance and southern Gulf of California. LPZ, influenced by oligotrophic and stratified Pacific waters, remains consistently low in productivity and can be dominated by picophytoplankton, whereas MPZ exhibits greater variability, particularly in winter, when nutrient enrichment enhances NPP.

At the seasonal scale, NPP peaks during winter (December–May), with maxima in February and March. This increase is driven by prevailing northwesterly winds and seasonal cooling that enhance upwelling along the eastern gulf coast, enriching the euphotic zone with nutrients and stimulating phytoplankton growth (Santamaria-del Angel et al., 1994; Escalante et al., 2013). Enhanced mixing during this period also reduces euphotic zone depth anomalies (EZDa, Fig. A5), reflecting increased phytoplankton biomass and reduced light penetration associated with productive conditions. During winter, HPZ and MPZ together cover ~77 % of the gulf. (Hakspiel-Segura et al., 2022) reported a negative correlation between SST and surface Chl-a, as well as between meridional wind stress and Chl-a in the central gulf, reinforcing the role of wind-driven mixing.

Conversely, during the warm season (June–November), oligotrophic conditions dominate, with NPP < 900 mg C m^{-2} d^{-1} covering ~68 % of the gulf. These conditions result from weak southeasterly winds, the intrusion of warm tropical waters, and strong stratification that limits nutrient supply (Lavin-Peregrina and Marinone-Moschetto, 2003; Escalante et al., 2013; Mercado-Santana et al., 2017; Trasviña-Castro et al., 2024).

The 2003–2024 NPP time series exhibited pronounced interannual variability. A significant negative correlation was found between the MEI v2 and HPZ coverage ($r_s(264) = -0.21$, $p < 0.05$). MEI v2 showed negative anomalies during 2006–2009, 2010–2012, and 2020–2022, corresponding to La Niña events. These periods were characterized by lower SST, intensified northwesterly winds, and a deeper mixing layer, which enhanced nutrient concentrations (NO_3, PO_4, and SiO_2) in the euphotic zone and increased NPP.

In 2008, 2011, 2012, and 2021, corresponding to moderate to strong La Niña phases, HPZ accounted for > 70 % of total NPP and covered 35–44 % of the gulf. Seasonality was most evident in winter, when HPZ and MPZ together covered ~95 % of the gulf, displacing LPZ to the mouth (Fig. A1).

Consistent with this physical mechanism, the stratification index (SI) analysis revealed distinct stratification regimes corresponding to each productivity zone (Fig. A8): HPZ exhibited consistently low SI values (0–0.5 kg m^{-3}), indicating well-mixed conditions maintained by persistent upwelling, tidal forcing, and winter wind-driven mixing. In contrast, LPZ displayed the

https://doi.org/10.5194/egusphere-2026-1040
Preprint. Discussion started: 10 March 2026

highest SI (~2.0 kg m^{-3}), characteristic of strongly stratified oligotrophic waters. MPZ typically showed intermediate and variable SI (0.5–1.1 kg m^{-3}), reflecting its transitional nature.

This mechanistic link was particularly evident from mid-2013 onward, when positive SST anomalies, increased stratification, and reduced nutrient concentrations (NO_3, PO_4) triggered persistent negative NPP anomalies, shifting pelagic habitat toward warm, oligotrophic conditions (Fig. A4–Fig. A7). This pattern reflects global trends of warming and stratification documented in the North Atlantic, North Pacific, and other regions (Xie et al., 2019; Fischer et al., 2020; Honda, 2020; Sanchez-Cabeza et al., 2022), which impact hydrographic structure, primary productivity, phytoplankton functional composition, and coastal carbon fluxes (Xie et al., 2019; Fischer et al., 2020; Honda, 2020; Hakspiel-Segura et al., 2022; Song et al., 2022).

The 2014–2016 period represents a tipping point in NPP variability in the Gulf of California, encompassing the most intense negative anomalies of the entire time series. Unlike shorter warm events, this episode resulted from the convergence of high-frequency atmospheric forcing (MEI v2), low-frequency climate modes (a positive PDO and the transition to a negative NPGO), and the simultaneous occurrence of marine heatwaves, which collectively amplified impacts on the physical and biogeochemical structure of the system, consistent with (Hakspiel-Segura et al., 2022).

The persistent increase in SST during 2014–2016 was the primary negative control on NPP, reducing winter HPZ coverage to < 5 % and expanding LPZ to ~50 % of the gulf. SST anomalies exceeding $+2°$ C intensified thermal stratification, reduced mixed-layer depth, and limited nutrient transport into the euphotic zone. These effects were particularly evident in the HPZ and MPZ, where productivity typically relies on the interaction between vertical mixing, coastal upwelling, and tidal forcing (Di Lorenzo and Mantua, 2016; Hakspiel-Segura et al., 2022).

Additionally, the SI revealed that this spatial reorganization was driven by a basin-wide intensification of stratification (Fig. A8). During this period, SI increased by approximately 60–80 % relative to its long-term mean, reaching values typically associated with oligotrophic conditions (> 1.5 kg m^{-3}) and rendering MPZ "LPZ-like" in its physical structure. Even HPZ exhibited enhanced stratification, although it remained within mixing-favorable values. This pervasive increase in stratification, particularly the "oligotrophication" of MPZ, created a widespread physical barrier to vertical nutrient flux, directly explaining the observed PO_4 declines and contraction of productive habitat.

A second key mechanism was the weakening of northwesterly winds during the winters of 2014–2016. The reduction in wind stress (~ 8 m s^{-1} compared with climatological values > 20 m s^{-1}) diminished the efficiency of coastal upwelling along the eastern continental margin. As a result, the characteristic winter fertilization of the gulf was substantially attenuated, shifting the seasonal productivity maximum and reducing HPZ coverage during the winter of 2015–2016. Simultaneously, the intrusion of Tropical Surface Water reinforced stratification and limited mesoscale activity, particularly in the southern gulf and at the mouth (Di Lorenzo et al., 2008, 2013; Di Lorenzo and Mantua, 2016).

This period recorded the lowest NPP of the entire record, with HPZ and MPZ contributions declining by ~7 % and coverage decreasing 5–10 % below historical averages. HPZ persisted only in the upper gulf (Fig. A3), while MPZ shifted northward and LPZ expanded by ~6 %, reaching latitudes up to 27° N (Fig. A2). The combined influence of warm, low-salinity, and nutrient-poor waters further restricted vertical exchange and sustained low-productivity conditions.

https://doi.org/10.5194/egusphere-2026-1040
Preprint. Discussion started: 10 March 2026

Additionally, nutrient data indicate that the reduction in NPP during 2014–2016 was not solely a thermal response. A marked decline in PO_4 concentrations was observed within the upper 100 m of the water column (Fig. A7), especially in HPZ and MPZ, suggesting N–P co-limitation (Browning and Moore, 2023). This finding highlights a more prominent role of phosphorus in regulating productivity in the gulf during extreme warm events than traditionally assumed.

Long-term trends indicate a decline in NPP of 50–100 mg C m^{-2} d^{-1} in the upper gulf and along the Sonora and Nayarit coasts (Fig. A9), while values at the mouth and in the central gulf (~28° N) remained relatively stable. This pattern mirrors global trends reported by (Maishal, 2024a, b), who documented a ~25 mg C m^{-2} d^{-1} per decade decline in the Pacific Ocean associated with warming of 0.1–0.2° C per decade, rates slightly lower than those reported for the Gulf of California (0.38 and 0.57° C per decade; (Hakspiel-Segura et al., 2022; Sanchez-Cabeza et al., 2022)). (Maishal, 2024a) also noted concurrent decreases in water density, salinity, wind stress, mixed layer depth, and nutrient concentrations (NO_3, PO_4) over the past two decades, consistent with our findings.

Despite this long-term decline, NPP rebounded following the prolonged low-productivity phase of 2013–2019. Productivity recovered during 2020–2024, and although 2023—the warmest oceanic year on record (Cheng et al., 2024)—did not yield the lowest NPP (which occurred in 2016 at 85 Tg C y^{-1}), 2024 ranked fourth highest (152 Tg C y^{-1}), suggesting system resilience potentially associated with the negative phase of the PDO that began in late 2019.

Globally, inverse relationships between NPP, Chl-a, and ocean warming are well documented, along with strong coupling between NPP and climate variability (Behrenfeld et al., 2006; Xie et al., 2019; Fischer et al., 2020; Honda, 2020). Positive phases of climate indices such as MEI v2 and PDO suppress NPP through warm-water intrusion, enhanced stratification, and oligotrophication. These processes alter atmospheric pressure centers and wind regimes, reducing upwelling intensity and nutrient supply.

This study advances our understanding of the regional and seasonal mechanisms affecting NPP in the Gulf of California, primarily mediated by SST and its associated processes. The integration of long-term environmental datasets demonstrates the utility of satellite-based and model-derived observations for detecting variability in NPP. Our parsimonious classification into three NPP zones (HPZ, MPZ, LPZ) effectively captures spatial and temporal heterogeneity. Further research is needed to elucidate the drivers of LPZ expansion observed over the past decade and to assess its potential ecological and socioeconomic consequences.

5 Conclusions

The average total NPP in the Gulf of California during 2003–2024 was 124 Tg C y^{-1}. Classification of the Gulf of California into three NPP categories using the k-means++ algorithm provided an effective and parsimonious framework for explaining spatial and temporal variability in NPP. HPZ conditions prevailed along the continental coast and the Midriff Archipelago, contributing 61.4 % of total NPP while covering ~30 % of the gulf's area. In contrast, LPZ conditions dominated the oceanic region and the gulf mouth, covering ~36 % of the area and contributing 16.9 % of total NPP.

https://doi.org/10.5194/egusphere-2026-1040
Preprint. Discussion started: 10 March 2026

The 2014–2016 period demonstrates that the decline in NPP in the Gulf of California resulted from the nonlinear interaction among surface warming (El Niño), weakened wind forcing, tropical water intrusion, intensified thermal stratification, reduced nutrient supply, and marine heatwaves. This coupling explains both the magnitude of the productivity collapse and the unprecedented expansion of oligotrophic conditions observed during these years.

Seasonal variability was pronounced: the cold season (December–May) accounted for 68 % of annual NPP, while the warm season (June–November) contributed 32 %. GLMM analysis revealed that SST was the dominant driver of NPP across all zones. In HPZ, NPP was additionally influenced by EZD, MLD, and PO_4 concentrations. Warmer years were associated with reduced coverage of productive zones (HPZ and MPZ) and expansion of oligotrophic LPZ areas.

As regional warming and stratification trends persist, oligotrophic conditions and low productivity are likely to intensify, extending LPZ influence further into the gulf. These changes could have significant ecological and socioeconomic consequences, underscoring the need for continued monitoring and research to anticipate, understand, and mitigate the impacts of climate variability on marine productivity.

Data availability. The datasets supporting the findings of this study are openly available in Zenodo at https://doi.org/10.5281/zenodo.18776942

Appendix A: Supplementary figures

Author contributions. Conceptualization: EGR, RCD; Data curation: EGR; Formal analysis: EGR, RCD, JDAA; Investigation: EGR, RCD; Methodology: EGR, JDAA; Project administration: EGR, RCD; Supervision: EGR, RCD, JDAA, JGG; Validation: RCD; Visualization: EGR, JDAA; Writing–original draft: EGR, RCD, JDAA; Writing – review & editing: EGR, RFC, JDAA, JGG.

Competing interests. The contact author has declared that none of the authors has any competing interests

Financial support. This research was supported by an internal project from CICESE-UALP awarded to EGR [project number 691110], Instituto Politécnico Nacional (IPN-SIP grant Multidisciplinary projects 2020–2022, 2023–2025), and the National Council of Science and Technology (CONACYT) currently known as Secretaria de Ciencia, Humanidades, Tecnología e Innovación (SECIHTI) [CF-6364]. JDA-A deeply thanks SECIHTI for the postdoctoral grant given in 2025–2026, RCD and JGG for EDI-IPN and COFAA-IPN grants and all authors for their SNII fellowship.

https://doi.org/10.5194/egusphere-2026-1040
Preprint. Discussion started: 10 March 2026

Acknowledgements. We thank National Space Administration (NASA) Ocean Biology Processing Group (OBPG), Copernicus Marine Environment Monitoring Service (https://marine.copernicus.eu/node/169), and National Oceanic and Atmospheric Administration (NOAA) (https://psl.noaa.gov/enso/mei/) for data set availability. We also thank MacTavish Scientific Editing for English translation services.

https://doi.org/10.5194/egusphere-2026-1040
Preprint. Discussion started: 10 March 2026

References

Alvarez-Borrego, S.: Flujos de carbono en los Golfos de California y Mexico, in: Carbono en Ecosistemas Acuaticos, edited by Hernandez-de-la Torre, B. and Gaxiola-Castro, G., pp. 337–353, Centro de Investigacion Cientifica y de Educacion Superior de Ensenada (CICESE), Ensenada, Baja California, Mexico, ISBN 978-968-817-855-3, 2007.

Alvarez-Borrego, S.: New phytoplankton production as a tool to estimate the vertical component of water exchange between the Gulf of California and the Pacific, Ciencias Marinas, 38, 89–99, https://doi.org/10.7773/cm.v38i1a.1885, 2012.

Alvarez-Borrego, S. and Lara-Lara, J. R.: The physical environment and primary productivity of the Gulf of California, in: The Gulf of California and Peninsular Province of the Californias, edited by Dauphin, J. P. and Simoneit, B. R., pp. 555–567, American Association of Petroleum Geologists, 1991.

Badan-Dangon, A., Koblisnksy, C. J., and Baumgartner, T.: Spring and summer in the Gulf of California: Observations of surface thermal patterns, Oceanologica Acta, 8, 13–22, 1985.

Behrenfeld, M. and Falkowski, P.: Photosynthetic rates derived from satellite-based chlorophyll concentration, Limnology and Oceanography, 42, 1–20, https://doi.org/10.4319/lo.1997.42.1.0001, 1997.

Behrenfeld, M. J., O'Malley, R. T., Siegel, D. A., McClain, C. R., Sarmiento, J. L., Feldman, G. C., and Boss, E. S.: Climate-driven trends in contemporary ocean productivity, Nature, 444, 752–755, https://doi.org/10.1038/nature05317, 2006.

Browning, T. J. and Moore, C. M.: Global analysis of ocean phytoplankton nutrient limitation reveals high prevalence of co-limitation, Nature Communications, 14, 5014, https://doi.org/10.1038/s41467-023-40774-0, 2023.

Bustos-Serrano, H. and Castro-Valdez, R.: Flux of nutrients in the Gulf of California: Geostrophic Approach, Marine Chemistry, 99, 210–219, https://doi.org/10.1016/j.marchem.2005.09.012, 2006.

Cavole, L. M., Demko, A. M., Diner, R. E., Giddings, A., Koester, I., Pagniello, C. M. L. S., Paulsen, M. L., Ramirez-Valdez, A., Schwenck, S. M., Yen, N. K., Zill, M. E., and Franks, P. J. S.: Biological impacts of the 2013–2015 warm-water anomaly in the Northeast Pacific: winners, losers, and the future, Oceanography, 29, 273–285, https://doi.org/10.5670/oceanog.2016.32, 2016.

Cepeda-Morales, J., Gaxiola-Castro, G., Beier, E., and Godinez, V. M.: The mechanisms involved in defining the northern boundary of the shallow oxygen minimum zone in the eastern tropical Pacific Ocean off Mexico, Deep-Sea Research Part I: Oceanographic Research Papers, 76, 1–12, https://doi.org/10.1016/j.dsr.2013.02.004, 2013.

Cheng, L., Abraham, J., Trenberth, K. E., et al.: New Record Ocean Temperatures and Related Climate Indicators in 2023, Advances in Atmospheric Sciences, 41, 1068–1082, https://doi.org/10.1007/s00376-024-3378-5, 2024.

Di Lorenzo, E. and Mantua, N.: Multi-year persistence of the 2014/15 North Pacific marine heatwave, Nature Climate Change, 6, 1042–1047, https://doi.org/10.1038/nclimate3082, 2016.

Di Lorenzo, E., Schneider, N., Cobb, K. M., Franks, P. J., Chhak, K., Miller, A. J., McWilliams, J., Bograd, S., Arango, H., Curchitser, E., Powell, T., and Riviere, P.: North Pacific Gyre Oscillation links ocean climate and ecosystem change, Geophysical Research Letters, 35, L08 607, https://doi.org/10.1029/2007GL032838, 2008.

Di Lorenzo, E., Combes, V., Keister, J., Strub, P. T., Thomas, A., Franks, P., and Parada, C.: Synthesis of Pacific Ocean climate and ecosystem dynamics, Oceanography, 26, 68–81, https://doi.org/10.5670/oceanog.2013.76, 2013.

Escalante, F., Valdez-Holguin, J. E., Alvarez-Borrego, S., and Lara-Lara, J. R.: Temporal and spatial variation of sea surface temperature, chlorophyll a, and primary productivity in the Gulf of California, Ciencias Marinas, 39, 203–215, https://doi.org/10.7773/cm.v39i2.2233, 2013.

https://doi.org/10.5194/egusphere-2026-1040
Preprint. Discussion started: 10 March 2026

Fiedler, P. C. and Talley, L. D.: Hydrography of the eastern tropical Pacific: A review, Progress in Oceanography, 69, 143–180, https://doi.org/10.1016/j.pocean.2006.03.008, 2006.

Fischer, A. D., Hayashi, K., McGaraghan, A., and Kudela, R. M.: Return of the "age of dinoflagellates" in Monterey Bay: Drivers of dinoflagellate dominance examined using automated imaging flow cytometry and long-term time series analysis, Limnology and Oceanography, 65, 2125–2141, https://doi.org/10.1002/lno.11443, 2020.

Froelicher, T. L., Fischer, E. M., and Gruber, N.: Marine heatwaves under global warming, Nature, 560, 360–364, https://doi.org/10.1038/s41586-018-0383-9, 2018.

Garcia-Fernandez, F., Gomez-Gutierrez, J., De Silva-Davila, R., Hakspiel-Segura, C., Ambriz-Arreola, I., Martinez-Lopez, A., and Robinson, C. J.: Interannual response of euphausiid community abundance during the anomalous warming period (2014–2016) in the Gulf of California, Progress in Oceanography, 212, 102 994, https://doi.org/10.1016/j.pocean.2023.102994, 2023.

Gaxiola-Castro, G., Garcia-Cordova, J., Valdez-Holguin, J. E., and Botello-Ruvalcaba, M.: Spatial distribution of chlorophyll alpha and primary productivity in relation to winter physical structure in the Gulf of California, Continental Shelf Research, 15, 1043–1059, https://doi.org/10.1016/0278-4343(94)00071-T, 1995.

Greene, C., Thirumalai, K., Kearney, K., Delgado, J. M., Schwanghart, W., Wolfenbarger, N., Thyng, K., Gwyther, D., Gardner, A., and Blankenship, D.: The Climate Data Toolbox for MATLAB, Geochemistry, Geophysics, Geosystems, 20, 3774–3781, https://doi.org/10.1029/2019GC008392, 2019.

Hakspiel-Segura, C., Martinez-Lopez, A., Delgado-Contreras, J., Robinson, C. J., and Gomez-Gutierrez, J.: Temporal variability of satellite chlorophyll-a as an ecological resilience indicator in the central region of the Gulf of California, Progress in Oceanography, 205, 102 825, https://doi.org/10.1016/j.pocean.2022.102825, 2022.

Heras-Sanchez, M. C., Valdez-Holguin, J. E., Garatuza-Payan, J., Cisneros-Mata, M., Diaz-Tenorio, L. M., Robles-Morua, A., and Hazas-Izquierdo, R. G.: Regiones del golfo de California determinadas por la distribucion de la temperatura superficial del mar y la concentracion de clorofila-a, Biotecnia, 23, 13–21, https://doi.org/10.18633/biotecnia.v21i1.808, 2019.

Hidalgo-Gonzalez, R. M. and Alvarez-Borrego, S.: Total and new production in the Gulf of California estimated from ocean color data from the satellite sensor SeaWiFS, Deep-Sea Research Part II, 51, 739–752, https://doi.org/10.1016/j.dsr2.2004.05.006, 2004.

Hobday, A. J., Alexander, L. V., Perkins, S. E., Smale, D. A., Straub, S. C., Oliver, E. C. J., Benthuysen, J. A., Burrows, M. T., Donat, M. G., Feng, M., Holbrook, N. J., Moore, P. J., Scannell, H. A., Gupta, A. S., and Wernberg, T.: A hierarchical approach to defining marine heatwaves, Progress in Oceanography, 141, 227–238, https://doi.org/10.1016/j.pocean.2015.12.014, 2016.

Honda, M. C.: Effective vertical transport of particulate organic carbon in the Western North Pacific Subarctic Region, Frontiers in Earth Science, 8, 366, https://doi.org/10.3389/feart.2020.00366, 2020.

Intergovernmental Oceanographic Commission: The International Thermodynamic Equation of Seawater – 2010: Calculation and Use of Thermodynamic Properties, UNESCO, Paris, France, 1 edn., https://www.teos-10.org/pubs/TEOS-10_Manual.pdf, 2010.

Jacox, M. G., Hazen, E. L., Zaba, K. D., Rudnick, D. L., Edwards, C. A., Moore, A. M., and Bograd, S. J.: Impacts of the 2015–2016 El Nino on the California Current system: Early assessment and comparison to past events, Geophysical Research Letters, 43, 7072–7080, https://doi.org/10.1002/2016GL069716, 2016.

Jimenez-Quiroz, M. C., Cervantes-Duarte, R., Funes-Rodriguez, R., Baron-Campis, S. A., Garcia-Romero, F. J., Hernandez-Trujillo, S., Hernandez-Becerril, D. U., Gonzalez-Armas, R., Martell-Dubois, R., Cerdeira-Estrada, S., Fernandez-Mendez, J. I., Gonzalez-Ania, L. V., Vasquez-Ortiz, M., and Barron-Barraza, F. J.: Impact of "The Blob" and "El Nino" warming phenomena in the

https://doi.org/10.5194/egusphere-2026-1040
Preprint. Discussion started: 10 March 2026

SW Baja California peninsula: Plankton and environmental variability of Bahia Magdalena, Frontiers in Marine Science, 6, 25, https://doi.org/10.3389/fmars.2019.00025, 2019.

Joh, Y. and Di Lorenzo, E.: Evidence for stronger and more prolonged Northeast Pacific marine heatwaves, Geophysical Research Letters, 44, 11 663–11 671, https://doi.org/10.1002/2017GL075930, 2017.

Johnson, R. A. and Wichern, D. W.: Applied Multivariate Statistical Analysis, Pearson, 6 edn., 2018.

Jones, T., Parrish, J. K., Peterson, W. T., Bjorkstedt, E. P., Bond, N. A., Ballance, L. T., Bowes, V., Hipfner, J. M., Burgess, H. K., Dolliver, J. E., Lindquist, K., Lindsey, J., Nevins, H. M., Robertson, R. R., Roletto, J., Wilson, L., Joyce, T., and Harvey, J.: Massive mortality of a planktivorous seabird in response to a marine heatwave, Geophysical Research Letters, 45, 3193–3202, https://doi.org/10.1002/2017GL076164, 2018.

Kahru, M., Marinone, S. G., Lluch-Cota, S. E., Pares-Sierra, A., and Mitchell, G. B.: Oceancolor variability in the Gulf of California: Scales from days to ENSO, Deep-Sea Research Part II, 51, 139–146, https://doi.org/10.1016/j.dsr2.2003.04.001, 2004.

Kapoor, A. and Singhal, A. A.: Comparative Study of K-Means, K-Means++ and Fuzzy C-Means Clustering Algorithms, in: 3rd International Conference on Computational Intelligence & Communication Technology (CICT), pp. 1–6, Ghaziabad, India, https://doi.org/10.1109/ciact.2017.7977272, 2017.

Kobayashi, S., Ota, Y., Harada, Y., Ebita, A., Moriya, M., Onoda, H., Onogi, K., Kamahori, H., Kobayashi, C., Endo, H., Miyaoka, K., and Takahashi, K.: The JRA-55 Reanalysis: general specifications and basic characteristics, Journal of the Meteorological Society of Japan, 93, 5–48, https://doi.org/10.2151/jmsj.2015-001, 2015.

Kushnir, Y.: Interdecadal variations in North Atlantic sea surface temperature and associated atmospheric conditions, Journal of Climate, 7, 141–157, https://doi.org/10.1175/1520-0442(1994)007<0141:IVINAS>2.0.CO;2, 1994.

Lavin, M. F., Castro, R., Beier, E., and Godinez, V. M.: Mesoscale eddies in the southern Gulf of California during summer: Characteristics and interaction with the wind stress, Journal of Geophysical Research: Oceans, 118, 1367–1381, https://doi.org/10.1002/jgrc.20132, 2013.

Lavin-Peregrina, M. F. and Marinone-Moschetto, S. G. L.: An overview of the physical oceanography of the Gulf of California, in: Nonlinear Processes in Geophysical Fluid Dynamics, edited by Velasco-Fuentes, O. U., Sheinbaum, J., and Ochoa de la Torre, J. L., pp. 173–204, Kluwer Academic Publishers, https://doi.org/10.1007/978-94-010-0074-1_11, 2003.

Lluch-Cota, S. E., ed.: Gulf of California, PICES Special Publication, Sidney, Canada, 2004.

Lluch-Cota, S. E., Aragon-Noriega, E. A., Arreguin-Sanchez, F., et al.: The Gulf of California: Review of ecosystem status and sustainability challenges, Progress in Oceanography, 73, 1–26, https://doi.org/10.1016/j.pocean.2007.04.00, 2007.

Lopez-Martinez, J., Farach Espinoza, E. B., Herrera Cervantes, H., and Garcia Morales, R.: Long-term variability in sea surface temperature and chlorophyll a concentration in the Gulf of California, Remote Sensing, 15, 4088, https://doi.org/10.3390/rs15164088, 2023.

Maishal, S.: Decadal changes in global Oceanic Primary Productivity and its drivers, Ocean-Land-Atmosphere Research, 3, 0066, https://doi.org/10.34133/olar.0066, 2024a.

Maishal, S.: Unraveling the declining Indian ocean primary productivity and key drivers, Discover Ocean, 1, 17, https://doi.org/10.1007/s44289-024-00018-5, 2024b.

Marin-Enriquez, E., Cruz-Escalona, V. H., Enriquez-Garcia, A. B., and Felix-Ortiz, J. A.: Physical geographic regions in the Gulf of California defined using unsupervised learning algorithms, Regional Studies in Marine Science, 80, 103 923, https://doi.org/10.1016/j.rsma.2024.103923, 2024.

https://doi.org/10.5194/egusphere-2026-1040
Preprint. Discussion started: 10 March 2026

Martínez-López, A., Hakspiel-Segura, C., Robinson, C. J., and Gómez-Gutiérrez, J.: Winter picoplankton composition, abundance, and vertical distribution in the Midriff islands and central regions of the Gulf of California, Regional Studies in Marine Science, 63, 103 000, https://doi.org/10.1016/j.rsma.2023.103000, 2023.

Mercado-Santana, J. A., Santamaria-del Angel, E., Gonzalez-Silvera, A., Sanchez-Velasco, L., Gracia-Escobar, M. F., Millan-Nunez, R., and Torres-Navarrete, C.: Productivity in the Gulf of California large marine ecosystem, Environmental Development, 22, 18–29, https://doi.org/10.1016/j.envdev.2017.01.003, 2017.

Merrifield, M. A. and Winant, C. D.: Shelf circulation in the Gulf of California: A description of the variability, Journal of Geophysical Research, 94, 18 133–18 160, https://doi.org/10.1029/JC094iC12p18133, 1989.

Millan-Nunez, E., Delgadillo-Hinojosa, F., Hakspiel-Segura, C., Torres-Delgado, E. V., Felix-Bermudez, A., Segovia-Zavala, J. A., and Munoz-Barbosa, A.: Phytoplankton composition and biomass under oligotrophic conditions in the Guaymas Basin (Gulf of California), Ciencias Marinas, 49, e3302, https://doi.org/10.7773/cm.y2023.3302, 2023.

Mills, K. E., Pershing, A. J., Brown, C. J., Chen, Y., Chiang, F. S., Holland, D. S., Lehuta, S., Nye, J., Sun, J., Thomas, A., and Wahle, R.: Fisheries management in a changing climate: Lessons from the 2012 ocean heat wave in the Northwest Atlantic, Oceanography, 26, 191–195, https://doi.org/10.5670/oceanog.2013.27, 2013.

Miranda-Alvarez, C., Gonzalez-Silvera, A., Santamaria-del Angel, E., Lopez-Calderon, J., Godinez, V. M., Sanchez-Velasco, L., and Hernandez-Walls, R.: Phytoplankton pigments and community structure in the northeastern tropical Pacific using HPLC-CHEMTAX analysis, Journal of Oceanography, 76, 91–108, https://doi.org/10.1007/s10872-019-00528-3, 2020.

Moore, D. and McCabe, G., eds.: Introduction to the Practice of Statistics, W. H. Freeman, 3 edn., 1999.

Morel, A. and Berthon, J. F.: Surface pigments, algal biomass profiles, and potential production of the euphotic layer: Relationships reinvestigated in view of remote-sensing applications, Limnology and Oceanography, 34, 1545–1562, https://doi.org/10.4319/lo.1989.34.8.1545, 1989.

Morel, A. and Maritorena, S.: Bio-optical properties of oceanic waters: A reappraisal, Journal of Geophysical Research: Oceans, 106, 7163–7180, https://doi.org/10.1029/2000JC000319, 2001.

Oliver, E. C. J., Benthuysen, J. A., Bindoff, N. L., Hobday, A. J., Holbrook, N. J., Mundy, C. N., and Perkins-Kirkpatrick, S. E.: The unprecedented 2015/16 Tasman Sea marine heatwave, Nature Communications, 8, 16 101, https://doi.org/10.1038/ncomms16101, 2017.

Oliver, E. C. J., Burrows, M. T., Donat, M. G., Sen-Gupta, A., Alexander, L. V., Perkins-Kirkpatrick, S. E., Benthuysen, J. A., Hobday, A. J., Holbrook, N. J., Moore, P. J., Thomsen, M. S., Wernberg, T., and Smale, D. A.: Projected marine heatwaves in the 21st Century and the potential for ecological impact, Frontiers in Marine Science, 6, 734, https://doi.org/10.3389/fmars.2019.00734, 2019.

O'Reilly, J. and Sherman, K.: Primary productivity patterns and trends, in: Large Marine Ecosystems: Status and Trends, edited by IOC-UNESCO and UNEP, pp. 91–99, United Nations Environment Programme, Nairobi, 2016.

Petatan Ramirez, D.: Propuesta de zonacion del Golfo de California con base en variables oceanograficas y distribucion de macroinvertebrados, Ph.D. thesis, Universidad Autonoma de Baja California Sur (UABCS), 2015.

Portela, E., Beier, E., Barton, E. D., Castro, R., Godinez, V., Palacios-Hernandez, E., Fiedler, P. C., Sanchez-Velasco, L., and Trasvina, A.: Water masses and circulation in the tropical Pacific off central Mexico and surrounding areas, Journal of Physical Oceanography, 46, 3069–3081, https://doi.org/10.1175/JPO-D-16-0068.1, 2016.

Ramos-Rodriguez, A., Lluch-Cota, D. B., Lluch-Cota, S. E., and Trasvina-Castro, A.: Sea surface temperature anomalies, seasonal cycle and trend regimes in the Eastern Pacific coast, Ocean Science, 8, 81–90, https://doi.org/10.5194/osd-8-1215-2011, 2012.

https://doi.org/10.5194/egusphere-2026-1040
Preprint. Discussion started: 10 March 2026

Robles-Tamayo, C. M., Garcia-Morales, R., Valdez-Holguin, J. E., Figueroa-Preciado, G., Herrera-Cervantes, H., Lopez-Martinez, J., and Enriquez-Ocana, L. F.: Chlorophyll-a concentration distribution on the mainland coast of the Gulf of California, Mexico, Remote Sensing, 12, 1335, https://doi.org/10.3390/rs12081335, 2020.

Roden, G. I. and Emilsson, I.: Physical oceanography of the Gulf of California, Ph.D. thesis, Dissertation, Mexico, 1979.

Round, F. E.: The phytoplankton of the Gulf of California Part 1. Its composition, distribution and contribution to the sediments, Journal of Experimental Marine Biology and Ecology, 1, 76–97, 1967.

Sanchez-Cabeza, J. A., Herrera-Becerril, C. A., Carballo, J. L., Yanez, B., Alvarez-Sanchez, L. F., Cardoso-Mohedano, J. G., and Ruiz-Fernandez, A. C.: Rapid surface water warming and impact of the recent (2013–2016) temperature anomaly in shallow coastal waters at the eastern entrance of the Gulf of California, Progress in Oceanography, 202, 102 746, https://doi.org/10.1016/j.pocean.2022.102746, 2022.

Santamaria-del Angel, E., Alvarez-Borrego, S., and Muller-Karger, F. E.: Gulf of California biogeographic regions based on coastal zone color scanner imagery, Journal of Geophysical Research, 99, 7411–7421, https://doi.org/10.1029/93JC02154, 1994.

Somavilla, R., Gonzalez-Pola, C., and Fernandez-Diaz, J.: The warmer the ocean surface, the shallower the mixed layer. How much of this is true?, Journal of Geophysical Research: Oceans, 122, 7698–7716, https://doi.org/10.1002/2017JC013125, 2017.

Song, Y., Guo, Y., Liu, H., Zhang, G., Zhang, X., Thangaraj, S., and Sun, J.: Water quality shifts the dominant phytoplankton group from diatoms to dinoflagellates in the coastal ecosystem of the Bohai Bay, Marine Pollution Bulletin, 183, 114 078, https://doi.org/10.1016/j.marpolbul.2022.114078, 2022.

Trasviña-Castro, A., Torres-Hernandez, M. Y., Valle-Rodriguez, J. B., and Gonzalez-Rodriguez, E.: Interannual variability (2014–2016) of coastal mesoscale activity at the entrance of the Gulf of California as determined by remote sensing, Regional Studies in Marine Science, 77, 103 609, https://doi.org/10.1016/j.rsma.2024.103609, 2024.

Valdez-Holguin, J. E. and Lara-Lara, J. R.: Primary productivity in the Gulf of California: Effects of El Nino 1982–1983 event, Ciencias Marinas, 13, 34–50, https://doi.org/10.7773/cm.v13i2.533, 1987.

Wernberg, T., Bennett, S., Babcock, R. C., Bettignies, T., Cure, K., Depczynski, M., et al.: Climate-driven regime shift of a temperate marine ecosystem, Science, 353, 169–172, https://doi.org/10.1126/science.aad8745, 2016.

Wolter, K. and Timlin, M. S.: El Nino/Southern Oscillation behavior since 1871 as diagnosed in an extended multivariate ENSO index (MEI.ext), International Journal of Climatology, 31, 1074–1087, https://doi.org/10.1002/joc.2336, 2011.

Xie, F., Tao, Z., Zhou, X., Lv, T., and Wang, J.: Spatial and temporal variations of particulate organic carbon sinking flux in global ocean from 2003 to 2018, Remote Sensing, 11, 2941, https://doi.org/10.3390/rs11242941, 2019.

Zeitzchel, B.: Primary productivity in the Gulf of California, Marine Biology, 3, 201–207, https://doi.org/10.1007/BF00360952, 1969.

Zhang, Q. and Qian, J.: Identification and temporal distribution of typical rainfall types based on K-means++ clustering and probability distribution analysis, Hydrology, 12, 88, https://doi.org/10.3390/hydrology12040088, 2025.

Zhang, Z., Chen, X., Wang, C., Wang, R., Song, W., and Nie, F.: Structured multi-view k-means clustering, Pattern Recognition, 160, 111 113, https://doi.org/10.1016/j.patcog.2024.111113, 2025.

https://doi.org/10.5194/egusphere-2026-1040
Preprint. Discussion started: 10 March 2026

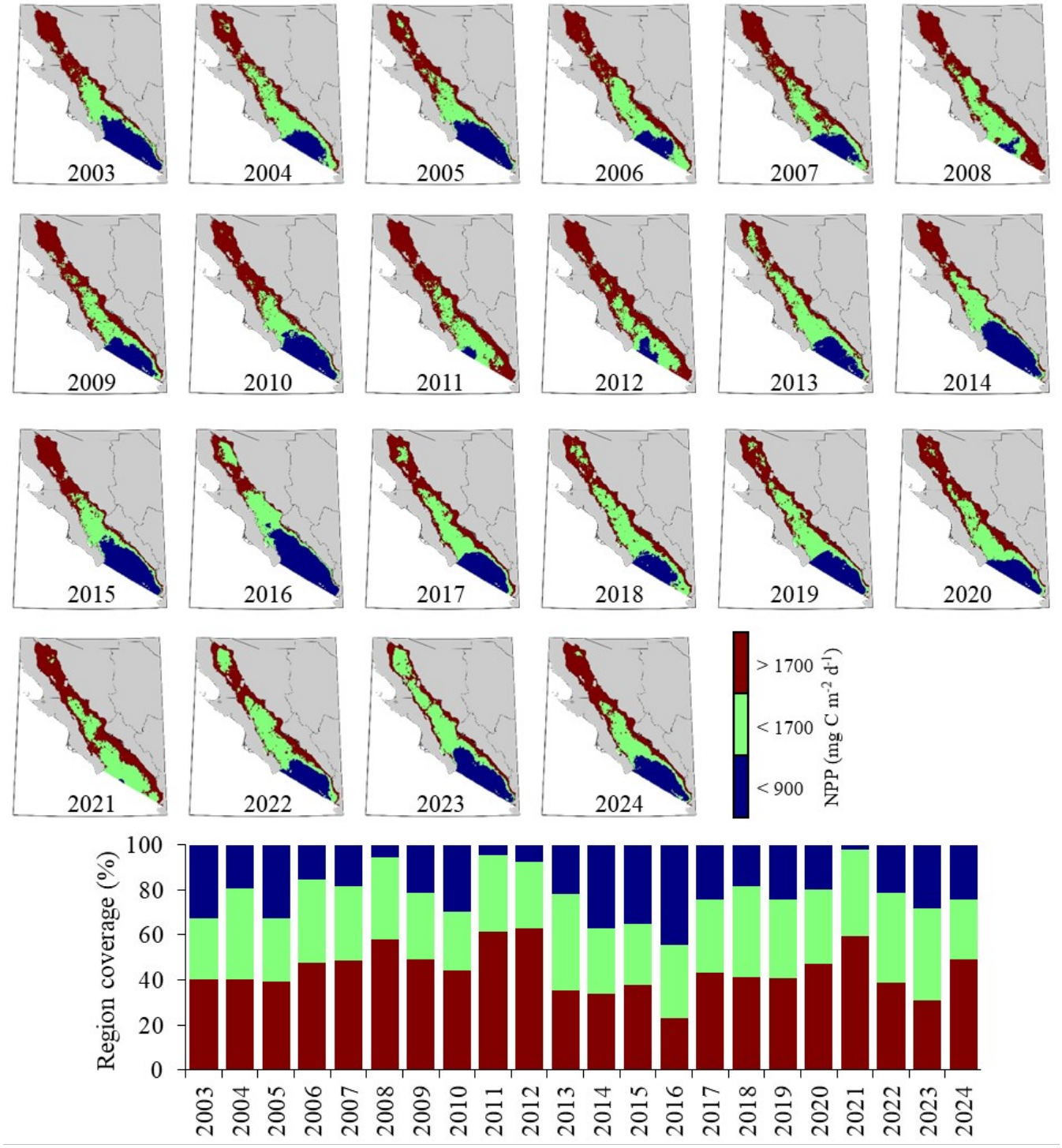

Figure A1. Spatial distribution of cold-season coverage (December–May) by productivity zone for each year from 2003 to 2024. Zones are defined as: high productivity zone (HPZ, >1700 mg C m^{-2} d^{-1}), mid productivity zone (MPZ, 900–1700 mg C m^{-2} d^{-1}), and low productivity zone (LPZ, <900 mg C m^{-2} d^{-1}).

https://doi.org/10.5194/egusphere-2026-1040
Preprint. Discussion started: 10 March 2026

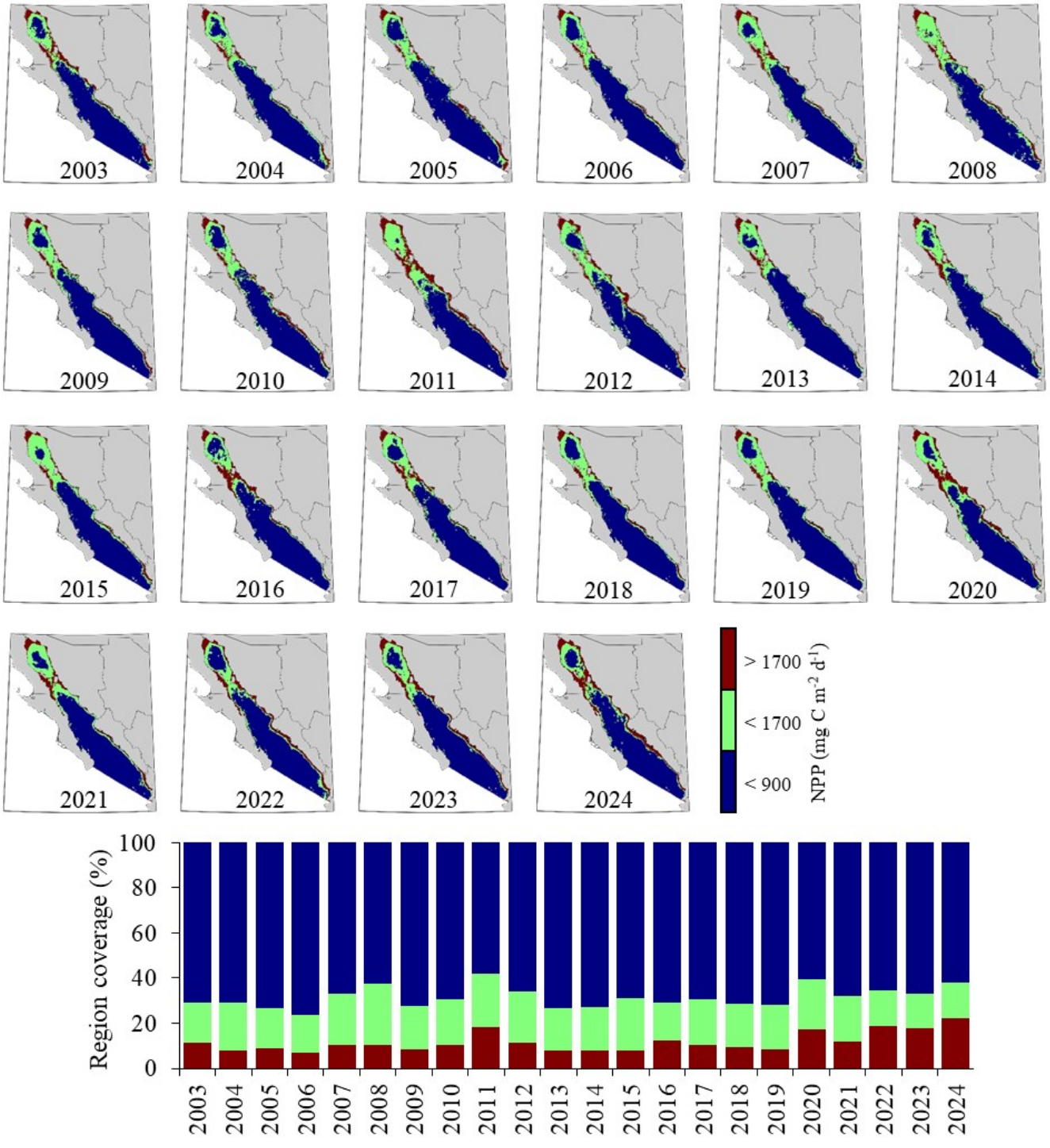

Figure A2. Spatial distribution of warm-season coverage (June–November) by productivity zone for each year from 2003 to 2024. Zones are defined as: high productivity zone (HPZ, >1700 mg C m^{-2} d^{-1}), mid productivity zone (MPZ, 900–1700 mg C m^{-2} d^{-1}), and low productivity zone (LPZ, <900 mg C m^{-2} d^{-1}).

https://doi.org/10.5194/egusphere-2026-1040
Preprint. Discussion started: 10 March 2026

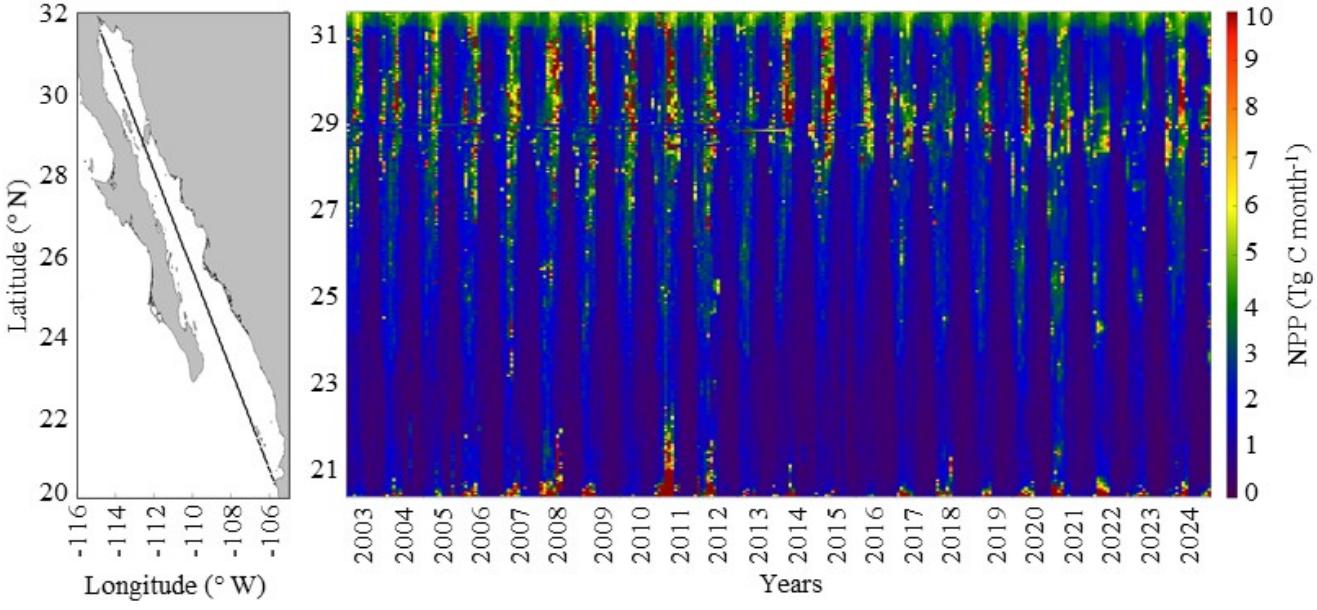

Figure A3. Monthly and latitudinal distribution of net primary productivity (NPP) in the central Gulf of California. The left panel shows the study area and the central-gulf transect used for analysis, while the right panel presents the corresponding Hovmöller diagram illustrating NPP variability over time.

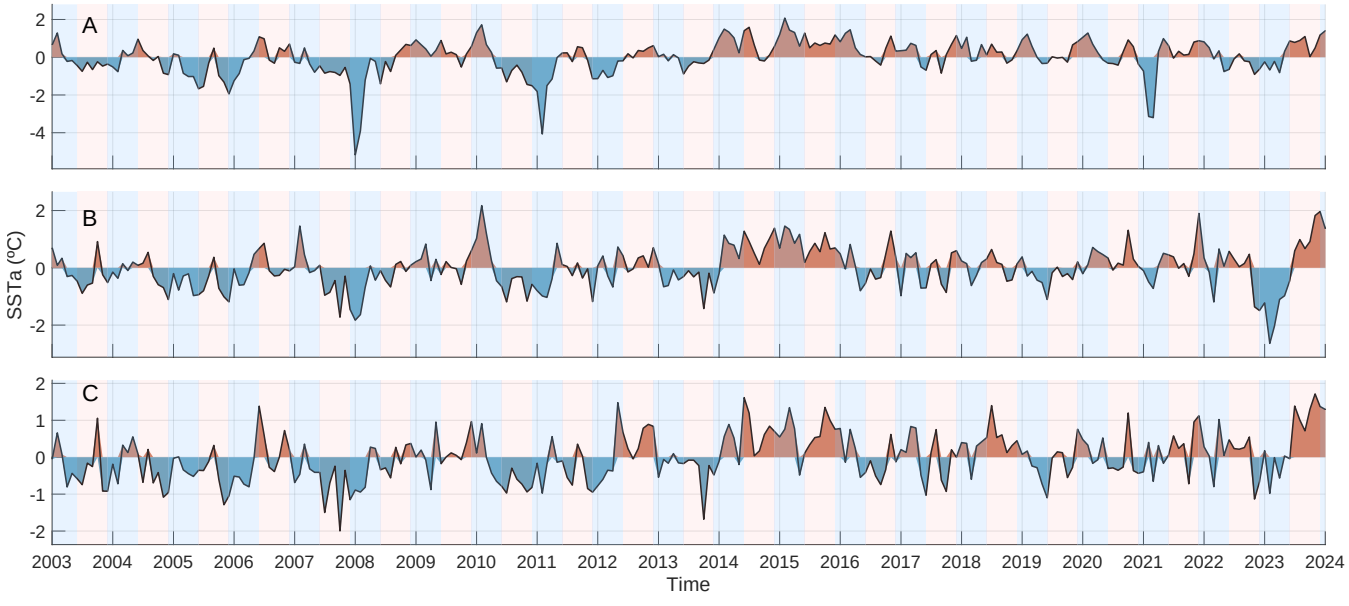

Figure A4. Sea surface temperature (SSTa) from 2003 to 2024 for (A) LPZ, (B) MPZ, and (C) HPZ. Positive values indicate a deepening of the euphotic zone, whereas negative values indicate shoaling. Alternating shaded bands denote cool and warm periods.

https://doi.org/10.5194/egusphere-2026-1040
Preprint. Discussion started: 10 March 2026

Figure A5. Euphotic zone depth anomalies (EZDa) from 2003 to 2024 for (A) LPZ, (B) MPZ, and (C) HPZ. Positive values indicate a deepening of the euphotic zone, whereas negative values indicate shoaling. Alternating shaded bands denote cool and warm periods.

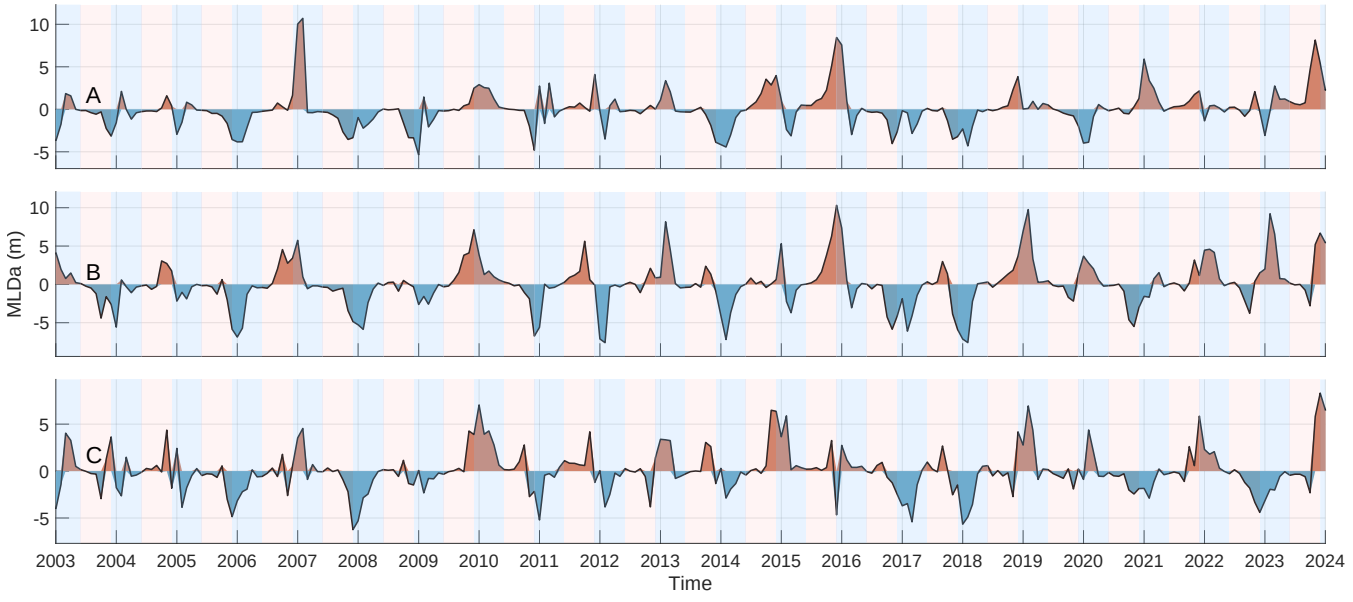

Figure A6. Mixed layer depth (MLDa) anomalies from 2003 to 2024 for (A) LPZ, (B) MPZ, and (C) HPZ. Positive values indicate a deepening of the euphotic zone, whereas negative values indicate shoaling. Alternating shaded bands denote cool and warm periods.

https://doi.org/10.5194/egusphere-2026-1040
Preprint. Discussion started: 10 March 2026

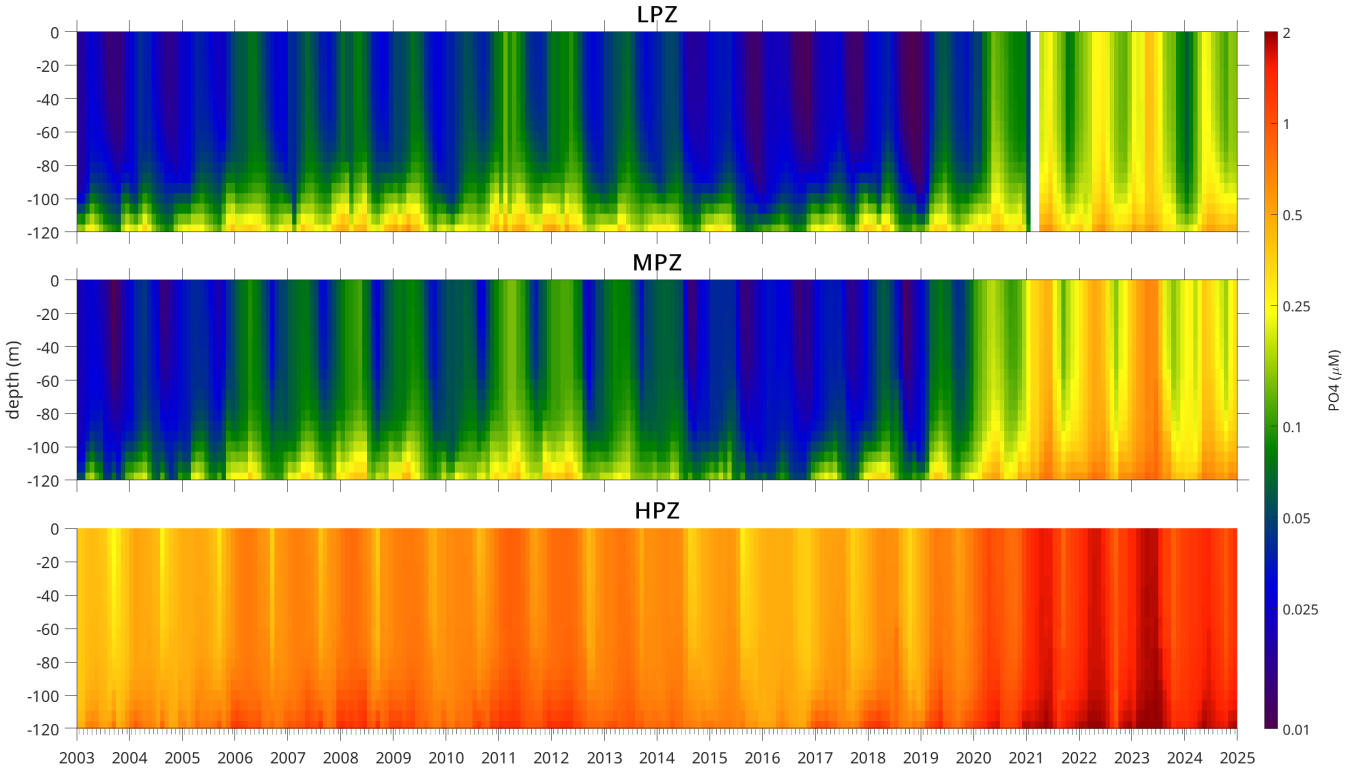

Figure A7. Vertical distribution of integrated phosphate (PO_4) by productivity zone and depth (0–120 m) during the study period (2003–2024). Panels from top to bottom correspond to LPZ, MPZ, and HPZ.

https://doi.org/10.5194/egusphere-2026-1040
Preprint. Discussion started: 10 March 2026

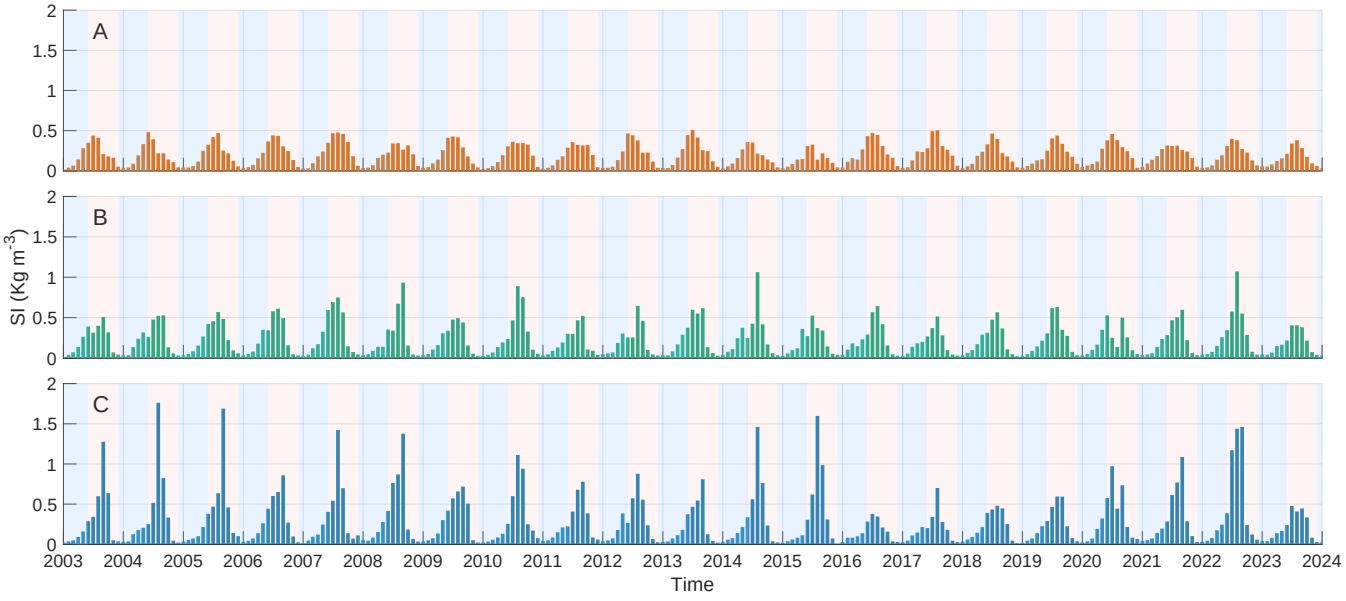

Figure A8. Stratification index (kg m^{-3}) during the study period (2003–2024). Panels from top to bottom correspond to (A) HPZ, (B) MPZ, and (C) LPZ. Alternating shaded bands denote cool and warm periods.

https://doi.org/10.5194/egusphere-2026-1040
Preprint. Discussion started: 10 March 2026

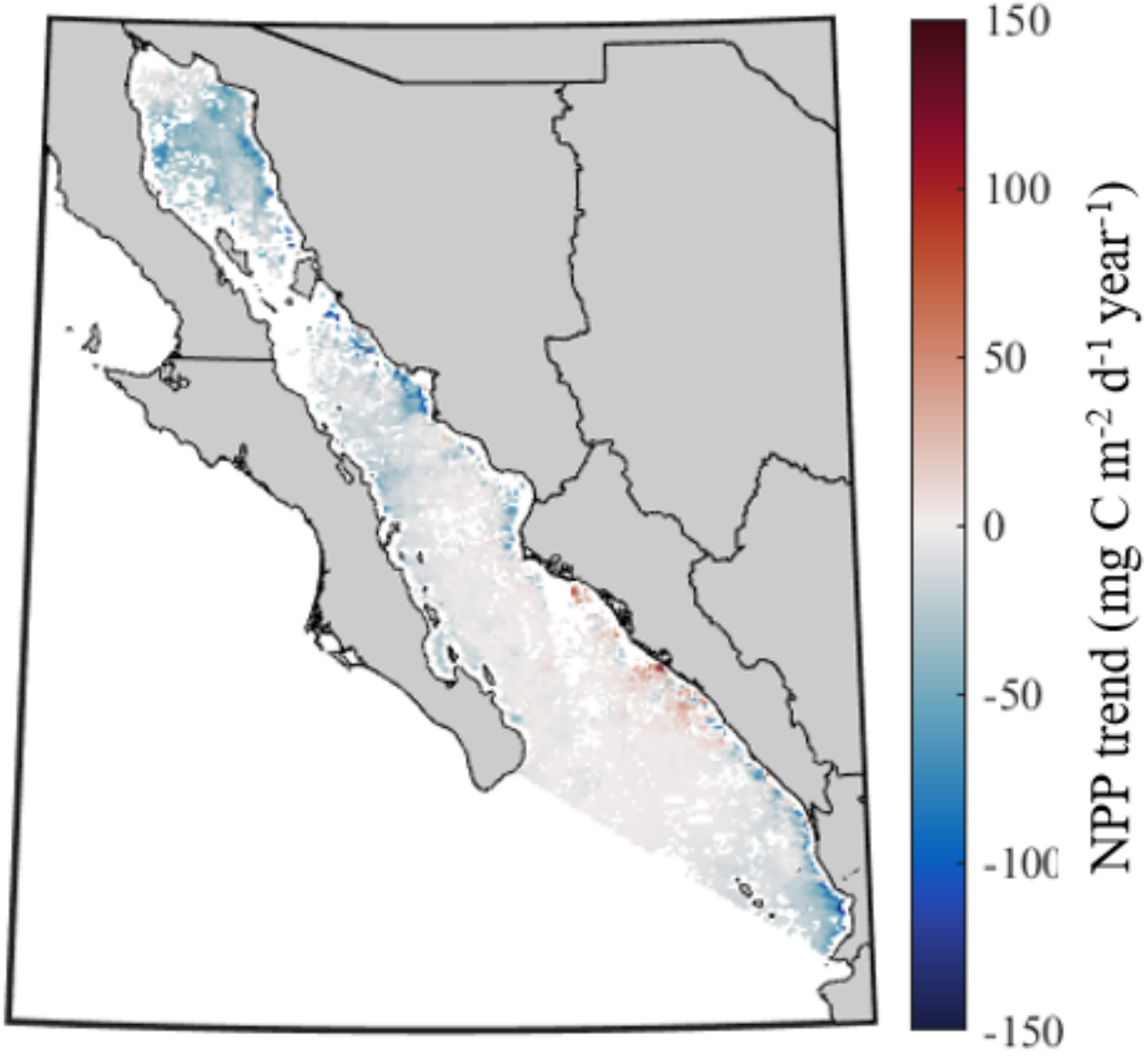

Figure A9. Spatial trend in net primary productivity (NPP; mg C m^{-2} d^{-1} yr^{-1}) across the Gulf of California during 2003–2024.